



GPR-Driven Geomechanical Modeling and Drill-Blast Optimization for Enhanced Efficiency in Open-Pit Gold Mining

Talgat Almenov ¹, Raissa Zhanakova ^{1*}, Mels Shautenov ¹, Guljan Askarova ²,
Nurdaulet Agybayev ³, Samal Assylkhanova ¹

¹ Satbayev University, Almaty, 50013, Kazakhstan.

² Al-Farabi Kazakh National University, Almaty, Kazakhstan.

³ Joint-Stock Company "Altynalmas", Almaty, Kazakhstan.

Received 07 July 2025; Revised 19 October 2025; Accepted 23 October 2025; Published 01 November 2025

Abstract

This study seeks to raise the operational efficiency and economic return of the Vasilkovskoye open-pit gold mine by integrating real-time ground-penetrating-radar (GPR) monitoring, geomechanical modeling, and digital optimization of drilling-and-blasting parameters. Continuous GPR scanning identified hazardous fracture zones that were subsequently characterized in DIPS and RS2 to model slope stability, while ShotPlus-based blast simulations and OrePro 3D displacement modeling guided the redesign of hole spacing, charge distribution, and delay timing. Fragmentation quality was verified with high-resolution photogrammetry and correlated to blast design through statistical analysis; a comparative techno-economic assessment quantified cost and dilution differentials between conventional and optimized schemes. The integrated workflow established a robust predictive link between blast geometry and fragment size, reducing oversize generation by 17% and ore dilution by 9%, while increasing gold grade in mill feed from 0.84 g t^{-1} to 0.94 g t^{-1} . GPR-informed hazard mapping eliminated unplanned wall failures, and the revised pattern lowered specific explosive consumption without compromising fragmentation, cutting total unit costs by 8%. Unlike previous studies that treat slope stability and blasting as separate tasks, this study couples deformation dynamics with blast design in a single digital loop, offering a transferable framework for automation-ready, risk-aware mine planning at complex geological sites.

Keywords: Open-Pit Gold Mining; Ground-Penetrating Radar (GPR); Drill-And-Blast Optimization; Geomechanical Modeling; Rock Fragmentation; Digital Mine Planning.

1. Introduction

In recent years, the gold mining industry has undergone significant changes due to growing global demand, geopolitical instability, and stricter sustainability requirements. In 2024, global demand for gold reached 4,974 tons, and central bank purchases exceeded 1,000 tons for the third consecutive year, contributing to gold prices rising above US\$ 3,500 per ounce by mid-2025 [1]. In response to these challenges, mining companies are increasingly turning to the development of deep, low-grade, and geologically complex deposits, where traditional drilling and blasting methods are becoming ineffective and economically unfeasible. The key technical challenge in such conditions is to optimize drilling and blasting operations, taking into account the high heterogeneity and tectonic disturbance of the rock mass. Studies show that inappropriate charging parameters that do not take into account structural anisotropy can lead to the formation of oversized rock, slope failure, increased seismic loads, and dilution [2-4]. These losses not only reduce recovery but

* Corresponding author: raissazhanakova@yandex.ru



<http://dx.doi.org/10.28991/CEJ-2025-011-11-010>



© 2025 by the authors. Licensee C.E.J, Tehran, Iran. This article is an open access article distributed under the terms and conditions of the Creative Commons Attribution (CC-BY) license (<http://creativecommons.org/licenses/by/4.0/>).

can also amount to several million US dollars per production cycle. In addition, uneven fragmentation negatively affects subsequent processing and reduces gold recoverability.

To overcome these problems, modern geophysical monitoring methods are increasingly being used, in particular ground-penetrating radar (GPR), which allows hidden tectonic disturbances and lithological boundaries to be detected in real time. The effectiveness of GPR in identifying fractured zones, especially in carbonate and metamorphic rocks, has been demonstrated in a number of studies [5, 6]. However, most industrial applications are fragmented and are not integrated with geomechanical modeling, charge optimization, and technical and economic assessment [7, 8].

Numerical methods for modeling slope stability and failure zones are being developed in parallel. For example, finite and discrete element methods are used to evaluate the mechanical response of anisotropic rock masses to various charging schemes [3, 9]. However, such calculations are rarely verified in operating quarries, and quantitative assessments of the influence of tectonic disturbances on fragmentation are practically absent. There is also a lack of work combining GPR data, geomechanical modeling, fragmentation prediction, and adaptive blast design into a single digital control system.

Some recent studies have begun to address these gaps. For example, Ullah et al. [11] and Zvarivadza et al. [12] proposed a comprehensive approach to characterizing the array using borehole GPR, rotary percussion drilling, and indentation tests. The author also identified the critical role of groundwater in distorting the GPR signal and proposed the use of special fluids with suitable dielectric permeability. Other researchers [12-14] developed a multimodal system for evaluating the effectiveness of destressing blasts, including GPR monitoring, well visualization, numerical modeling, and seismic risk indices, supported by IIoT infrastructure and machine learning methods.

Despite the progress achieved, the following scientific gaps remain:

- Insufficient integration of GPR with stress-strain state modeling and BVR parameters [4, 5];
- Lack of large-scale validation of numerical models in operating quarries [15];
- Limited number of quantitative studies on the influence of tectonic fault orientation on fragmentation [9, 16, 17];
- Insufficient technical and economic assessment of the effectiveness of digital approaches compared to traditional ones [18, 19].

This study aims to address these gaps by introducing an integrated digital methodology based on GPR at tectonically disturbed site №5 of the Vasilkovsky gold deposit, one of the largest open-pit mines in Kazakhstan.

The proposed approach includes:

- Continuous GPR monitoring using IDS GeoRadar;
- Stereographic and stress-strain analysis in DIPS and RS2 software environments;
- Optimization of charging parameters using ShotPlus Premier;
- Fragmentation prediction based on photogrammetry and OrePro 3D.

Field tests have confirmed the high efficiency of the system:

- 50% reduction in oversize material formation;
- Nearly 30% reduction in dilution;
- Increase in gold content in the feed ore from 0.84 to 0.94 g/t;
- Increase in the proportion of marketable ore from 87.9% to 97.49%;
- Elimination of slope collapses and reduction in specific mining costs.

For the first time in scientific literature, a quantitative relationship has been established between the orientation and displacement of tectonic faults and the granulometric composition after an explosion. This has made it possible to rethink the design of charges, taking into account the structural anisotropy of the rock mass. Thus, it has been demonstrated that slope stability and fragmentation are not isolated problems, but when integrated, they form a synergistic system for improving the efficiency, extraction, and safety of mining operations.

The remainder of the article includes: theoretical justification and software used; description of geological conditions and experimental setup; results of field tests and their interpretation; discussion of limitations, scientific novelty, and scalability of the proposed approach; and a conclusion with key findings and recommendations for future research.

The subsequent structure of the article is as follows:

The second chapter is dedicated to the object of research, encompassing the geological and geomechanical characteristics of the work area, as well as tectonic features that influence both slope stability and rock crushing quality.

The third chapter of this study provides a comprehensive overview of the research methodology employed. The document meticulously delineates the sequence of actions involved in GPR monitoring and displacement analysis (Stage 1), the forecasting and modelling of displacement vectors within the DIPS programme (Stage 2), the section-by-section modelling of drilling and blasting operations (Stage 3), and the methodology for assessing rock mass size to optimise enrichment processes (Stage 4).

The results of the study are contained in Chapter 4. The results of GPR monitoring are presented in Section 4.1; the results of modelling fracture directions in the DIPS programme are presented in Section 4.2; and the results of modelling drilling and blasting operations, including section-by-section modelling (4.3.1) and the installation of explosive charges with a preliminary analysis of the fractional composition of the rock mass (4.3.2), are presented in Section 4.3.

The fifth chapter is dedicated to the discussion of the results obtained. Section 5.1 provides a comparative analysis of the existing and proposed contour drilling methods for ensuring slope stability. Section 5.2 presents a thoroughgoing analysis of the research results, including the control of the natural size of the rock mass to optimise enrichment processes (5.2.1), as well as a comparative economic analysis and assessment of the impact of the proposed technology on gold production indicators, taking into account the reduction in dilution (5.2.2).

Chapter 6 summarises the results of the study, formulates key conclusions and summarises the scientific and practical results of the work. The study focuses on the significance of the established relationships between the orientation of tectonic faults, blasting parameters and the granulometric composition of the rock. In addition, it explores the potential of an integrated approach to increase slope stability, crushing efficiency and reduce dilution. The final section of the chapter provides a series of recommendations for the practical implementation of the proposed methodology, as well as directions for further research in related fields.

2. Research object

The Vasilkovskoye field is located 17 km north of the city of Kokshetau, the administrative center of the Akmola region of the Republic of Kazakhstan, and 320 km from the country's capital, Astana (Figure 1). The territory of the district is characterized by a high level of economic development and the presence of a developed industrial and transport infrastructure, which creates favorable conditions for mining operations.

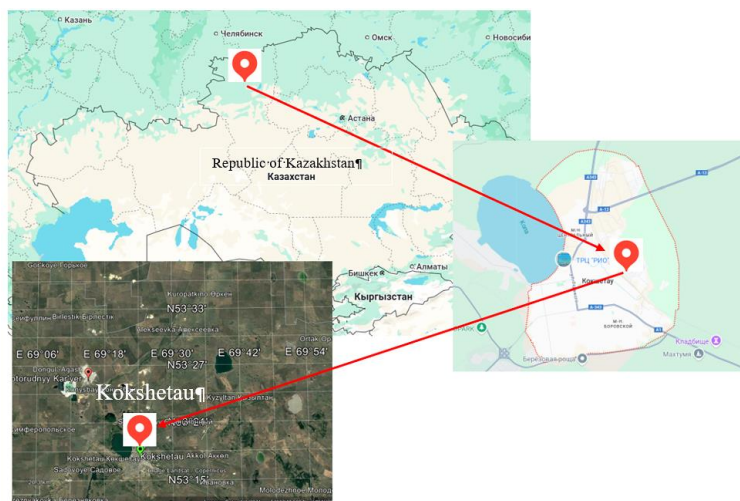


Figure 1. Location of the Kokshetau (gold deposit)

The industrial site has railroad branch line connection. Chaglinka railway station is located 14 km to the southeast of the field, and Kokshetau International Airport is located 30 km to the south. The field is connected to the nearest cities by republican highways with asphalt concrete and concrete coating, providing year-round transportation. The seismic activity in the area of the mining and processing enterprise ranges from 2 to 5 points according to SNiP RK 2.03-30-2006. The probability of strong earthquakes is considered extremely low, and natural hazardous geological processes such as avalanches or karst formations are not observed in the region.

The coordinates of the studied site are 49°01' N and 81°39' E, confined to the southwestern flank of the Donguliagash and Vasilkovo-Berezovsky regional faults. The geological structure consists of volcanogenic and sedimentary formations of the Bukonya Formation and effusive rocks of the Daubai Formation, including andesite-basalts. Tectonically, the deposit is situated in the hanging wall of the Vasilkovo-Berezovsky fault zone, within sandy-slate strata of the Bukonya Formation (Figure 1) [20]. The region is characterized by well-developed infrastructure, including roads, railways, energy supply, and water systems. The open-pit mine is designed with dimensions of 1,210 m in width, 1,290 m in length, and 450 m in depth. A gold processing plant meeting international standards operates on-site, with a

capacity of 8 million tons of ore per year and annual gold production of about 400-500 thousand troy ounces [2]. Ore mineralization is spatially associated with the lower horizon of bituminous hybrid lavas. Structural mapping confirms the presence of intense fracturing, especially in blocks bounded by large faults. The Vasilkovskoye deposit is located within the Altybai syncline, at the junction of the Donguliagash and north-eastern faults, marked by complex dislocation and faulting systems [21].

3. Research Methodology

To address the combined problems of pit-wall stability, blast performance and ore fragmentation, the study adopts a multi-scale, mixed-methods design that integrates in-situ geophysical monitoring with deterministic and stochastic modeling tools (Figure 2). This diagram reflects the research methodology of a step-by-step approach to achieving the required rock mass fragmentation (Figure 2). The presented process includes four key stages: radar monitoring and displacement analysis, fracture orientation modeling using DIPS software, drilling and blasting modeling, and rock size assessment to optimize enrichment processes. Sequential implementation of these stages ensures the achievement of the desired particle size distribution, which contributes to improving the efficiency of extracting useful components when developing structurally complex deposits.

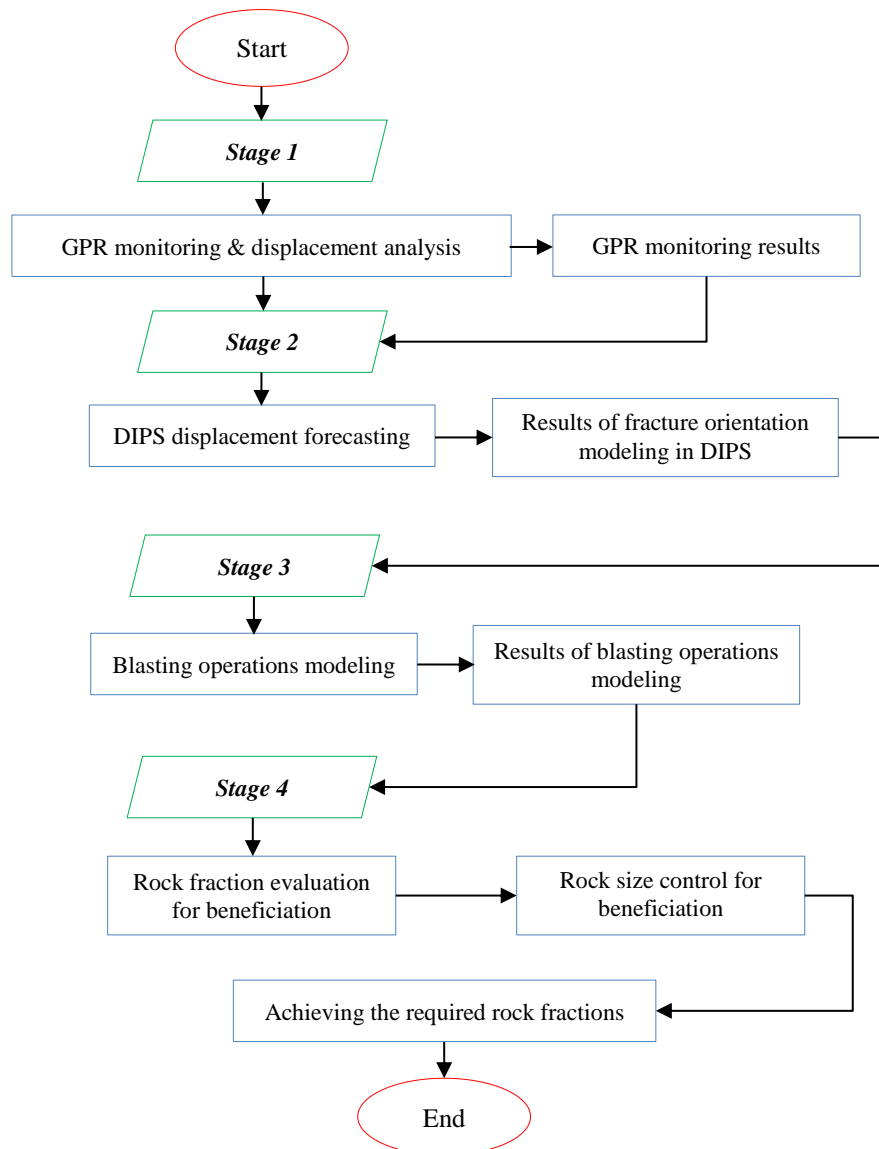


Figure 2. Research methods for a stepwise approach to achieving the required rock fractionation

Each methodological block is selected to close a specific knowledge gap identified in previous studies and is linked through a common data pipeline.

- **Systems analysis and theoretical synthesis:** A critical review of the mechanics of explosive rock breakage and pit-wall failure provides the conceptual backbone of the study, framing the principal variables, such as stress redistribution, joint orientation, charge energy and timing, that govern both safety and fragmentation outcomes [2, 20, 21]. The review informs the experimental design and the selection of monitoring and simulation parameters.

- **High-resolution geophysical monitoring:** Continuous, bench-scale imaging is performed with an FPM-360 ground-penetrating-radar array (400 MHz central frequency, 0.05 m point spacing) co-located with an IBIS-ArcSAR interferometric radar (range resolution < 0.5 mm). The dual-sensor configuration captures sub-meter fracture networks and real-time slope displacements at minute-scale intervals, thereby linking lithological heterogeneity to deformation kinetics [7, 22, 23]. These data constitute the primary boundary conditions for subsequent numerical models.
- **Structural interpretation and kinematic classification:** GPR-derived discontinuity sets are imported into DIPS 8.0, where stereographic projections and Markland kinematic tests quantify the likelihood of planar, wedge and toppling failures under current stress fields [8, 24]. The resulting polar density plots guide the assignment of anisotropic strength parameters in the finite-element models.
- **Geomechanical simulation under static and dynamic loads:** Bench-scale stability is modelled with RS2 (static, 2-D finite element) and FLAC3D (dynamic, 3-D explicit) to capture both steady excavation effects and blast-induced transients [3, 9]. Material properties are calibrated by back-analysis of radar-measured pre-blast displacements; model verification uses IBIS-ArcSAR records of post-blast wall response, providing a closed validation loop rarely reported in the literature.
- **Drill-and-blast design optimization:** Blast rounds are first parameterized in ShotPlus to explore alternative hole spacings, charge weights and delay patterns; stress wave outputs are then transferred to the calibrated FLAC3D grid to compute peak particle velocity fields and damage indices. The iteration process continues until the vibration and target fragmentation thresholds are reached simultaneously.
- **Fragmentation assessment and statistical reconciliation:** Post-blast muckpiles are surveyed with UAV-based photogrammetry; images are processed via split-merge algorithms to derive P-size distributions, which are regressed against predicted fragment sizes and energy inputs [4]. A two-sample Kolmogorov-Smirnov test evaluates whether modelled and observed distributions differ significantly at $\alpha = 0.05$.
- **Techno-economic evaluation:** Finally, production data from three consecutive benches are used to quantify the differences in gold-grade dilution and unit cost between baseline and optimized schemes. Sensitivity analysis separates the marginal contribution of each methodological component (GPR, kinematic filtering, dynamic stress modeling) to overall value creation.

The study provides a predictive validated workflow that can support real-time decisions by combining continuous geophysical data with mechanically consistent blast and stability models, promoting improvement over previous research that only addressed these issues separately.

This study presents a structured approach to achieving the target rock fraction (Figure 2), integrating GPR-based structural monitoring, geomechanical analysis, numerical modeling, and granulometric assessment. Initially, ground-penetrating radar is used to outline fracture zones and unstable areas, providing definition of rock mass boundaries and selection of extraction methods. Based on structural data and discontinuity analysis, potential displacement vectors are modelled to assess deformation risks during blasting. Numerical simulations are then used to determine optimal drilling and blasting parameters for the desired fragmentation. The final stage involves granulometric analysis through sampling and laboratory testing, with results compared to modelled outputs to assess process efficiency and adjust parameters for consistent yield of the target particle size (see Figure 3).

The block diagram (Figure 3) reflects an integrated step-by-step approach to obtaining a specified fraction of rock mass. The methodology includes the following sequential stages: monitoring the condition of the rock mass, modeling displacement directions, numerical modeling of drilling and blasting operations, and fractional analysis of actual particle size characteristics. At each stage, data is collected and processed to improve the accuracy of forecasting and optimize the crushing and enrichment processes. The presented structure provides a closed control system, where the results of each stage are used to adjust subsequent decisions in order to achieve the target parameters of the fractional composition.

To achieve the target rock fraction and optimize subsequent processing, a four-stage integrated approach was applied: monitoring, modeling, forecasting, and fractional analysis, each reflecting the geological and structural features of the deposit [16, 25, 26].

The first stage (Section 3.1) involves GPR scanning to identify zones of fracturing and local displacements affecting rock stability and crushing efficiency. The resulting radargrams and geophysical sections support the identification of unstable areas and inform further technological decisions [17, 27].

At the second stage (Section 3.2), structural modeling is performed using DIPS software, analyzing weakness planes and fracture orientations to forecast deformation trends and unstable blocks as key data for safe blast planning [28, 29].

The third stage (Section 3.3) includes numerical simulation of drilling and blasting, incorporating borehole geometry, explosive parameters, and timing schemes. The objective is to optimize rock fragmentation while minimizing over/under-crushing and predicting particle size distribution [30, 31].

The fourth stage (Section 3.4) focuses on quantitative analysis of rock coarseness, combining sampling, lab tests, and model validation. The results guide adjustments to blasting and processing to enhance beneficiation efficiency [32, 33].

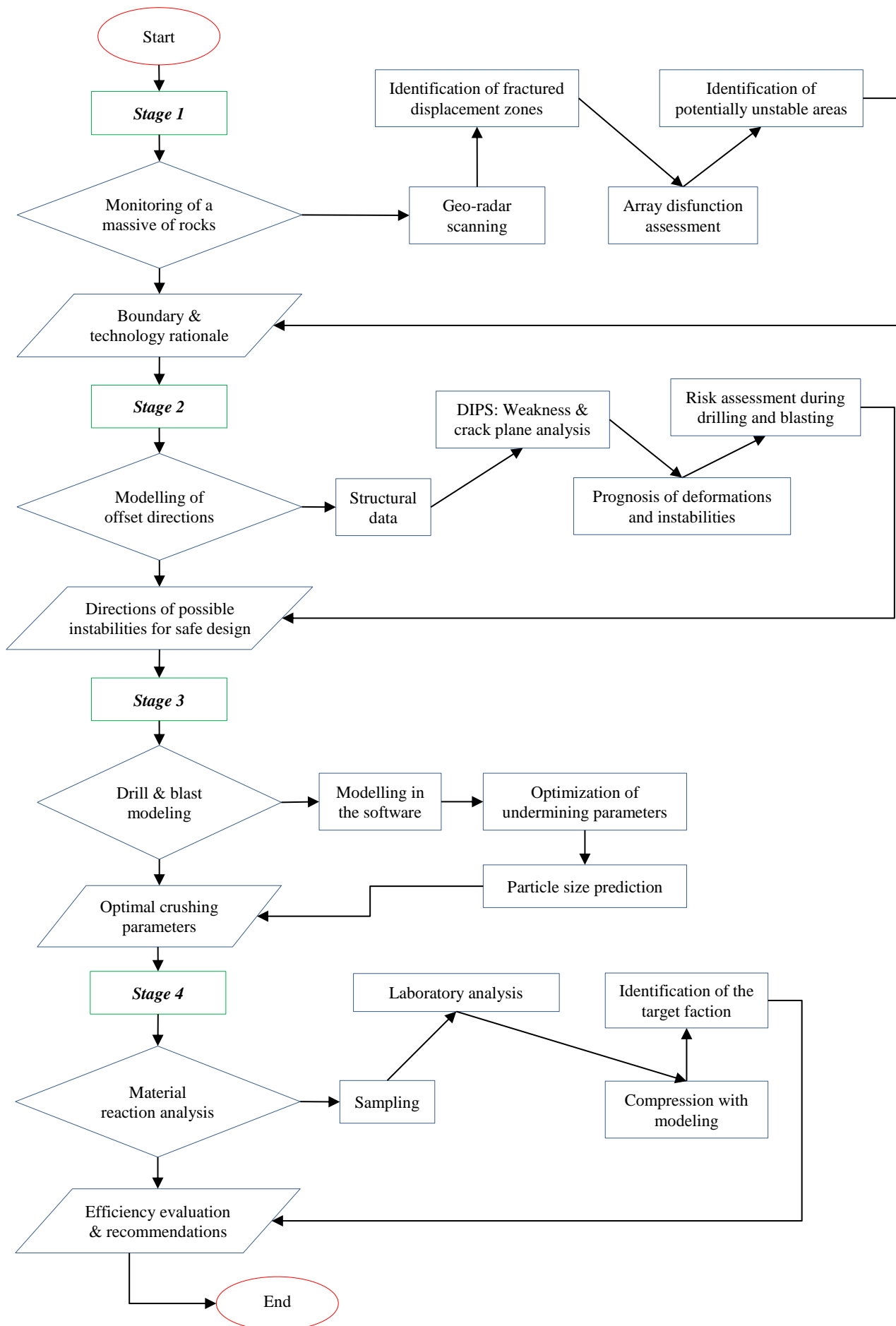


Figure 3. Block diagram of the integrated step-by-step approach to obtaining the target rock fraction

3.1. GPR Monitoring and Displacement Analysis (Stage 1)

Ground-penetrating radar (GPR) monitoring and displacement analysis are essential tools in ensuring the safety and efficiency of open-pit mining operations, where the risk of slope failure and geotechnical instability is high. The use of modern GPR systems provides timely and accurate data on the condition of the rock mass, enabling the identification of potentially hazardous zones and implementation of preventive measures. International mining practice demonstrates the effectiveness of such systems. For instance, quarries in Western Australia have successfully applied GPR technologies to prevent cave-ins, optimize blasting processes, and enhance operational safety [34]. Continuous monitoring enables early detection of unstable pit zones, adjustment of drilling and blasting parameters, and uninterrupted production flow.

GPR monitoring improves industrial safety and ore quality, particularly in gold mining. By detecting tectonic faults and highly fractured zones, it becomes possible to more accurately model rock behavior during blasting and optimize fragmentation parameters, reducing ore loss and processing inefficiencies. GPR technologies provide detailed information on rock structure, deformation, and stability. They are especially important in tectonically active regions where real-time tracking of massif conditions is required. Monitoring includes the use of radar systems, seismic sensors, satellite and ground-based displacement trackers, and 3D modeling tools. The operational principle of GPR is based on emitting radio waves that penetrate rock layers and reflect from boundaries with differing physical properties. The resulting signals are processed to generate detailed images of the internal structure of the massif. GPR is used to assess slope stability, detect geological anomalies, monitor post-blast changes, and predict geodynamic events. Displacement analysis involves comparing current and previous GPR data to detect anomalies, evaluate deformation trends, and assess potential geotechnical risks to mining operations.

In this study, GPR surveying was carried out using an FPM-360 array (central frequency 400 MHz, depth penetration up to 15 m, horizontal resolution 0.05 m) along three benches in Section No. 5 of the Vasilkovskoye open pit. The results were verified using an IBIS-ArcSAR interferometric radar, which confirmed that zones of intense GPR signal scattering coincided with areas where pre-blast slope deformations exceeded 1.5 mm/day. The data obtained in Stage 1 were subsequently used as input for kinematic analysis in the DIPS program (Stage 2) and for assigning anisotropic strength parameters in blast simulations (Stage 3), ensuring a continuous link between monitoring and design stages.

3.2. Prediction and Modeling of Shifts and Displacements in the DIPS Program (Stage 2)

Modern geotechnical monitoring methods assess the current condition of rock masses and predict potential structural changes. Numerical models based on displacement and tectonic disturbance data help identify zones of instability and forecast the development of deformation processes.

To analyze tectonic faults, the *Structural Interface* module in RS2 is applied. This tool models contacts between geological elements considering fault geometry, mechanical properties, and possible displacements. Given that tectonic zones often feature intensified fracturing, parameters such as normal and shear fracture stiffness are introduced to simulate the mechanical behavior of contacts under stress conditions [30, 35].

For spatial analysis and prediction of unstable blocks, the DIPS software is applied. It creates stereographic projections, identifies critical discontinuity orientations, and assesses potential failure planes. With this, it is possible to:

- Model probable zones of collapse or shear;
- Forecast deformation evolution;
- Provide engineering recommendations for blasting and slope design.

Integrating these modeling tools improves mine safety by enabling informed decisions on pit wall stability, blasting strategies, and overall risk reduction.

In this study, structural data obtained from Stage 1 GPR monitoring — including fracture orientations, spacing, and identified fault zones — were imported into DIPS 8.0 for kinematic analysis. The stereographic projections were cross-checked with field measurements, ensuring consistency between geophysical interpretations and actual geological observations. Critical discontinuity sets identified in DIPS were subsequently used to assign anisotropic strength parameters in RS2 simulations, directly linking Stage 2 results to stability assessments and blast design in Stage 3. This integration allowed for a more accurate prediction of potential failure planes and improved the precision of drilling and blasting parameters, thereby reducing geotechnical risks and enhancing operational safety.

3.3. Drilling and Blasting Modeling (Stage 3)

Simulation of drilling and blasting operations is a key stage in the design of efficient and safe rock mass destruction. This process ensures optimal fragmentation, improves ore recovery, and reduces operational costs. In modern mining, modeling is performed using mathematical and numerical methods that predict rock behavior under explosive loading, allowing for precise parameter selection.

The modeling process includes several stages:

- Analysis of geotechnical conditions. Physical and mechanical properties of rocks, geological structures, and tectonic features are analyzed to determine the most effective charging and initiation parameters.
- Selection of charge parameters. Parameters such as explosive type, charge mass, hole diameter, depth, and initiation schemes are optimized based on modeling results to achieve uniform fragmentation and minimize over- or under-crushing.

Advanced computational techniques, such as finite element method (FEM), discrete element method (DEM), and hydrodynamic modeling, are used in ANSYS, FLAC3D, RS2, and DIPS software. These tools simulate blast wave propagation, stress distribution, and rock deformation, enabling:

- Fracture efficiency assessment. Depending on lithology and structural conditions, models predict crushing volume, fragmentation quality, and stress redistribution.
- Impact forecasting on adjacent zones. Simulation helps identify potential adverse effects like slope instability or unexpected displacements caused by incorrect blast design.

Integration of GPR data (e.g., from GPR A-22, A-11, IDS GeoRadar) significantly enhances the accuracy of modeling. These systems provide real-time information on fractures, faults, and zones of weakness. Their use in pre- and post-blast analysis helps adjust charge placement and initiation to prevent hazardous displacements. At the final stage, geotechnical data (stress fields, displacements, slope angles) are processed to develop a refined drilling and blasting passport. This includes optimal charge configuration and initiation sequencing. Thus, integrated modeling significantly enhances the safety and efficiency of blasting operations in mining practice, considering geotechnical, geophysical, and technological factors.

In this study, input parameters for blast simulations in Stage 3 were derived directly from Stage 2 kinematic analysis results, ensuring that discontinuity orientations, fault zone locations, and anisotropic strength values were accurately represented in the numerical models. The calibrated FLAC3D and RS2 models incorporated real GPR-derived structural data, enabling precise prediction of stress wave propagation and damage zones. Simulation outputs were cross-validated with post-blast GPR and IBIS-ArcSAR monitoring results to verify fragmentation quality and slope stability response. This iterative process allowed for real-time adjustment of hole patterns, charge weights, and delay timing, creating a closed feedback loop between modeling and field performance, and directly feeding optimized parameters into Stage 4 rock coarseness analysis.

3.4. Methodology for Estimating Rock Coarseness for Optimization of Beneficiation Processes (Stage 4)

Nowadays, modern technologies and sensors such as TruckMetrics are actively used in the systems of mining companies. These solutions form important elements for improving the efficiency, safety and optimization of mining and mineral processing. Systems that integrate advanced technologies (GPR, sensors, wireless networks and data analytics systems) provide continuous monitoring of the state of mining massifs, technological processes and equipment. This makes it possible to identify potential safety threats in a timely manner, and optimize work processes to improve efficiency and reduce costs. The use of specialized systems, such as TruckMetrics, provides monitoring of equipment operation, control of safety parameters, load profiling and production volume tracking [36]. These systems promptly perform video analysis with the use of artificial intelligence technologies, which enables quick responses to deviations in equipment operation and accelerates management decision-making processes (Figures 4 and 5).



Figure 4. The order of rock coarseness studies for optimization of beneficiation processes



Figure 5. Location of sensors for determining rock coarseness

Monitoring systems, such as BeltMetrics [37], are used to control product quality during the mineral processing stages. These technologies provide continuous assessment of particle size distribution and material quality, reducing the risk of end-product contamination and improving the overall efficiency of beneficiation processes. Despite the existence of modern technologies for assessing rock coarseness, such systems have not yet been introduced at the given field [16, 17, 32]. Therefore, photo-documentation remains the primary method for evaluating the quality of drilling and blasting operations and determining rock fragmentation. This method is integrated with GPR survey data and drilling and blasting parameters to optimize gold beneficiation processes [25, 27, 38].

Combining photo-documentation with GPR results provides a comprehensive understanding of changes in rock structure. Statistical analysis of the obtained data allows identifying patterns in rock fragmentation, predicting variations in material composition, and adjusting technological parameters to enhance beneficiation efficiency and reduce processing costs. The integration of photo-documentation with geophysical and blasting data significantly improves the accuracy of monitoring, enabling timely process optimization. Thus, photo-documentation becomes a key element in assessing the rock mass state, improving the efficiency and safety of gold ore processing.

In this study, Stage 4 rock coarseness analysis was carried out using field photo-documentation combined with Stage 3 optimized drilling and blasting parameters and structural data from Stage 1–2 monitoring. This integration allowed the measured particle size distributions from muckpiles to be directly compared with modelled fragmentation outputs, enabling validation of simulation accuracy and identification of deviations in field performance. The resulting feedback was used to refine blast design in subsequent cycles, ensuring consistent achievement of target size fractions and improved beneficiation efficiency. By closing the loop between monitoring, modeling, blasting, and coarse fraction assessment, Stage 4 provides the final control point in the methodology before operational adjustments are implemented.

The proposed research methodology follows an integrated, step-by-step approach designed to address the combined challenges of slope stability, blast performance, and optimal rock fragmentation in structurally complex gold deposits. The process is structured into four sequential stages, each informed by the results of the previous stage and contributing to a closed-loop system for continuous improvement.

Stage 1 involves ground-penetrating radar (GPR) monitoring and displacement analysis to identify fracture networks, tectonic faults, and unstable rock mass zones. This stage provides the structural and deformation baseline for all subsequent analyses.

Stage 2 focuses on prediction and modeling of displacement directions using the DIPS program. Structural data from Stage 1 are used to determine critical discontinuity sets and assign anisotropic strength parameters in geomechanical models, enabling accurate kinematic assessments of potential failure modes.

Stage 3 comprises drilling and blasting modeling in FLAC3D and RS2, calibrated with data from Stages 1 and 2 and verified against post-blast monitoring results. This step allows optimization of borehole geometry, charge configurations, and delay sequences to achieve the target fragmentation while minimizing adverse stability impacts.

Stage 4 involves rock coarseness assessment through field photo-documentation and integration of data from Stages 1–3. By comparing actual particle-size distributions with modeled outcomes, deviations can be detected, and blast parameters adjusted for consistent yield of the desired size fractions, improving beneficiation efficiency.

Together, these stages form a cohesive and data-driven methodology in which monitoring, modeling, blasting, and coarse fraction analysis are interlinked, ensuring both technical accuracy and operational efficiency in open-pit mining.

4. Results

4.1. Results of the GPR Monitoring Study

To achieve high performance in mining production, it is necessary to conduct preliminary geological studies and organize continuous monitoring of the pit condition during its operation. In the period from 2023 to 2024, intensive geotechnical monitoring was conducted at the considered site using GPR systems A-22 and A-11. These systems provide high-precision detection of potential safety threats, and prediction of possible displacements of the quarry sides, which, in turn, is an important factor for optimizing the parameters of drilling and blasting operations [2, 20, 21].

Geotechnical monitoring and displacement analysis are necessary tools to ensure safe and efficient mining operations. The use of GPR technologies, seismic sensors and other control methods makes it possible to monitor the condition of the massif and promptly forecast possible risks. Prospective development of technologies and integration of modern methods of analysis open new opportunities for improved accuracy, efficiency and safety of mining operations.

As a result of these studies, a sensitivity map was generated showing the directions of probable array displacements. This tool is an essential element for predicting changes in the geological state of the open pit and subsequent adjustment of drilling and blasting parameters to minimize geotechnical risks and improve the efficiency of production processes (Figure 6).

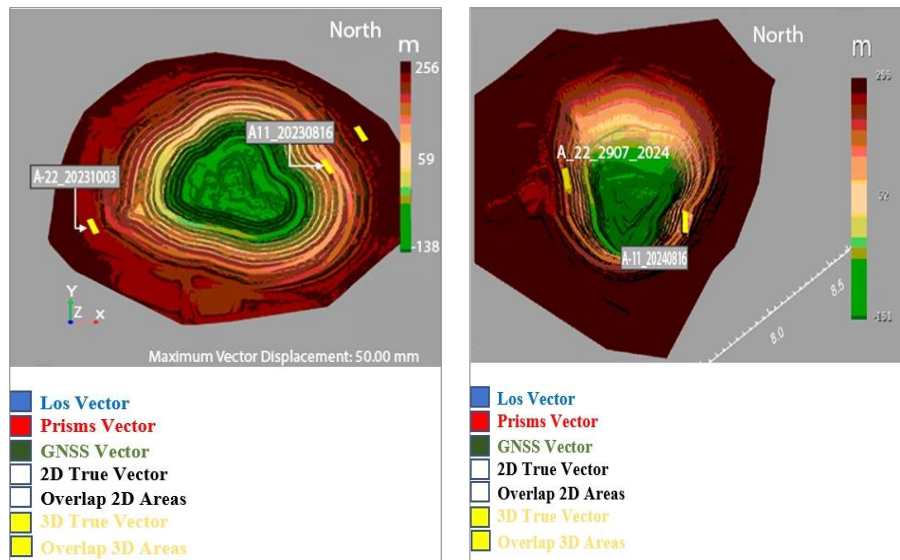
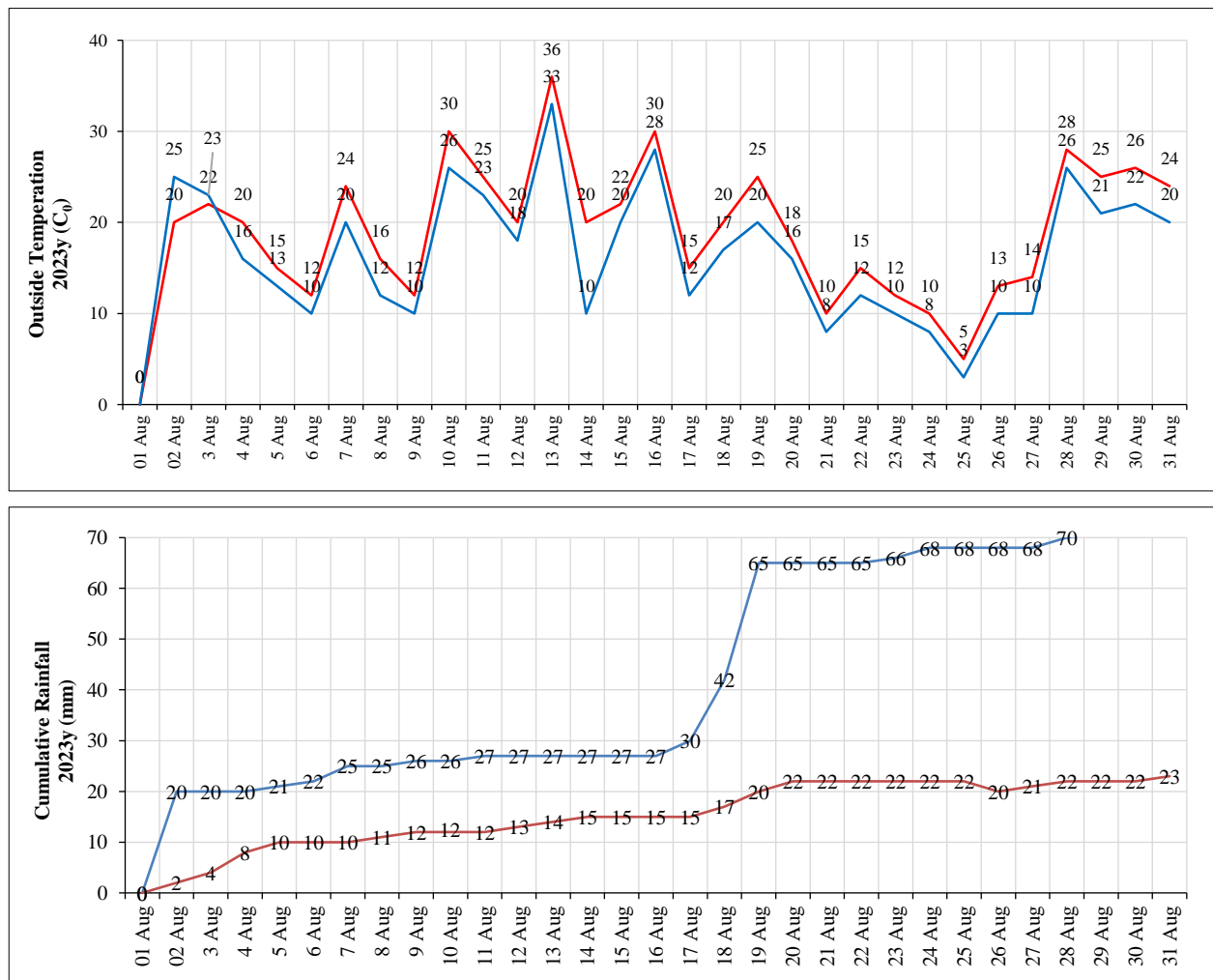


Figure 6. Location of radars, 2023-2024

The results of GPR surveys have identified several key areas that pose a potential threat to safe mining operations. Two years of monitoring revealed tectonic faults that significantly impact the stability of the pit sides. Thus, in 2023, the condition of one section of the scarp was classified as having a medium degree of stability. However, in 2024, based on repeated monitoring data, this section was categorized as hazardous. This fact demonstrates the need to promptly implement more accurate and well-founded engineering solutions aimed at optimizing drilling and blasting parameters and reducing geotechnical risks (Figures 7 and 8).



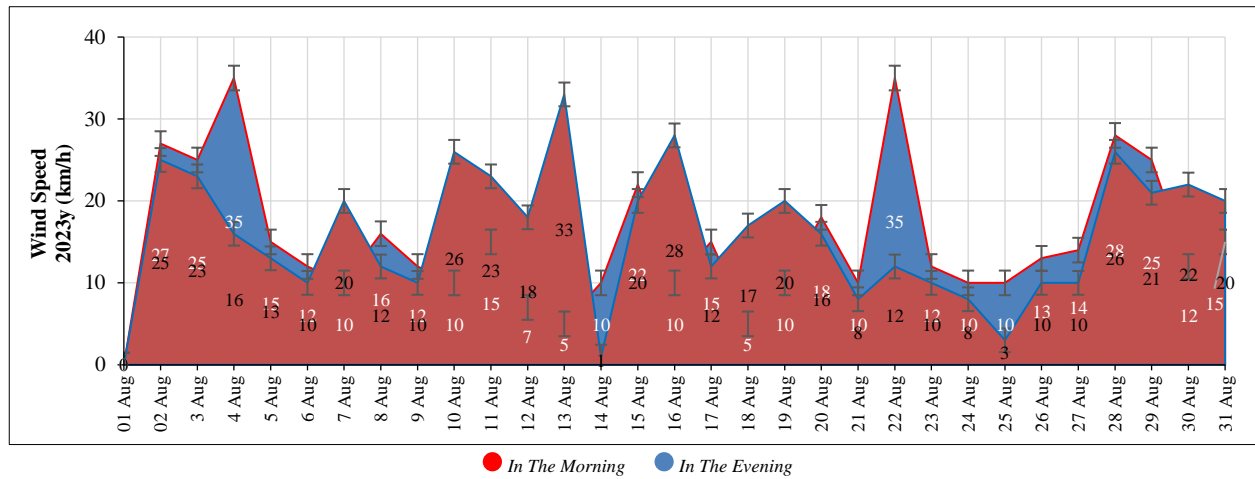


Figure 7. Results from weather reports for the period of 01.08.2023 - 31.12.2023 (August used as a representative example)

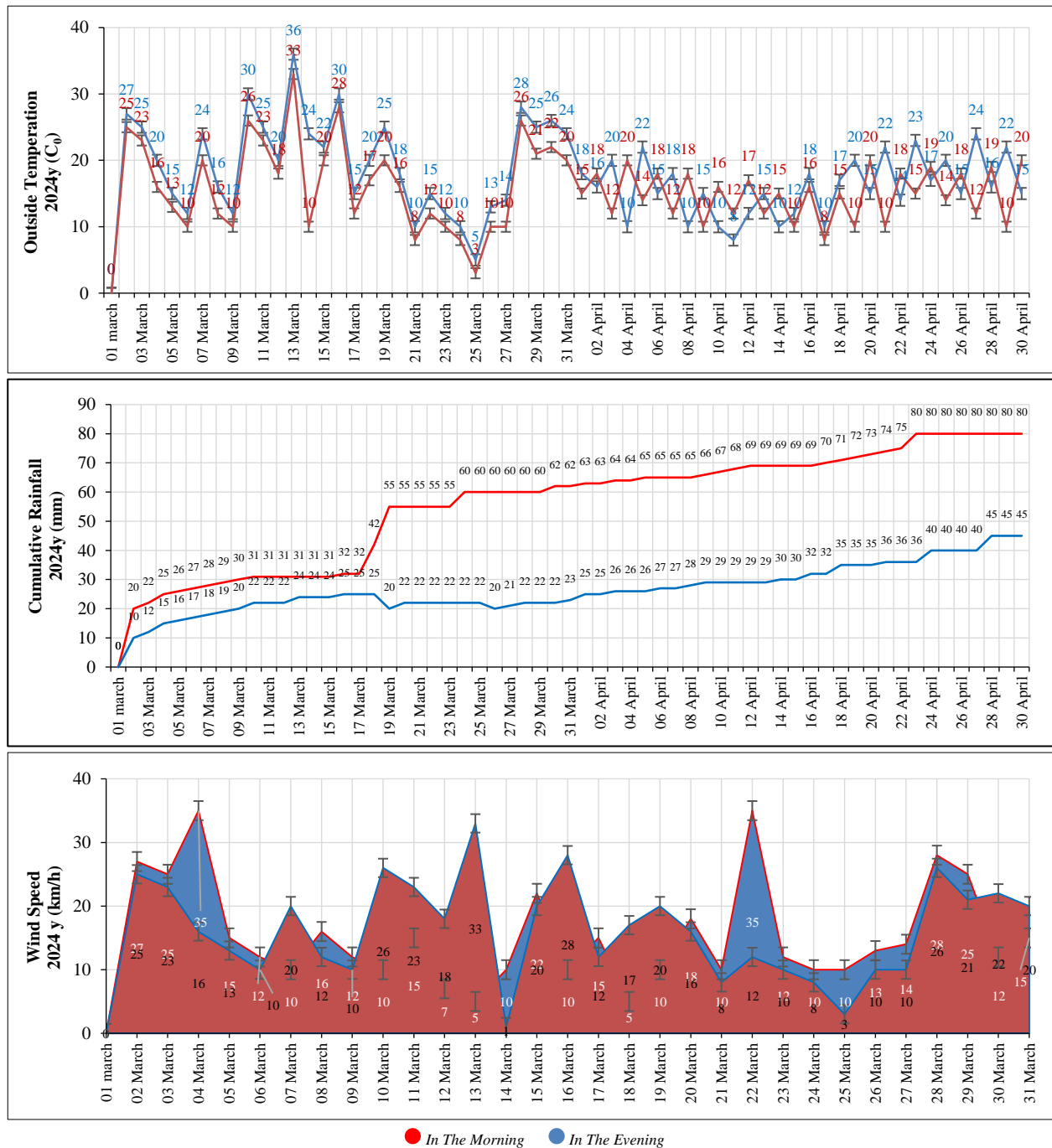


Figure 8. Results from weather reports for the period of 01.01.2024 - 31.05.2024 (March used as a representative example)

Figure 7 shows summary meteorological data for the period from August 1 to August 31, 2023, selected as a representative month for analyzing seasonal climatic factors affecting the stability of the array. The upper graph shows daily fluctuations in outdoor air temperature, demonstrating pronounced cycles with an amplitude of 20°C to 30°C. The middle graph shows accumulated precipitation, where two intense episodes of rainfall after August 18 are clearly visible. The bottom graph reflects wind speeds ranging from 5 to 25 km/h with peaks coinciding with periods of precipitation. The combination of these meteorological factors allows us to assess the impact of weather conditions on the intensification of displacements and slope instability in sector №5.

Figure 8 illustrates weather conditions for the period from March 1 to April 30, 2024, with March selected as a representative month for analyzing the climatic impact on the stability of the array. The upper diagram shows daily fluctuations in air temperature in the morning and evening hours, with an amplitude ranging from 5°C to 25°C. The middle graph shows accumulated precipitation, with marked stepwise increases after March 8, 15, and 28, indicating multiple episodes of rainfall. The bottom graph shows changes in wind speed, which on some days reached values above 40 km/h. The combination of these factors—temperature fluctuations, high humidity, and squally winds—creates conditions for the development of deformation processes, which is especially critical in the spring period with unstable geotechnical characteristics of the massif.

Next, we examine the sensitivity map, which can be used to analyze how well the GPR line of sight corresponds to the expected offset direction. This map is crucial when selecting alarm thresholds.

The range of the sensitivity map is $[0 \div 1]$.

- Sensitivity map value = 0: this is the lowest sensitivity (slope direction is mutually perpendicular to the GPR line of sight).
- Sensitivity map value = 1: this is the highest sensitivity (slope direction is parallel to the GPR line of sight).

The use of this map allows for prompt assessment of the conditions of GPR equipment operation and adjustment of the monitoring parameters depending on the geomechanically situation in the quarry (Figures 9 and 10).

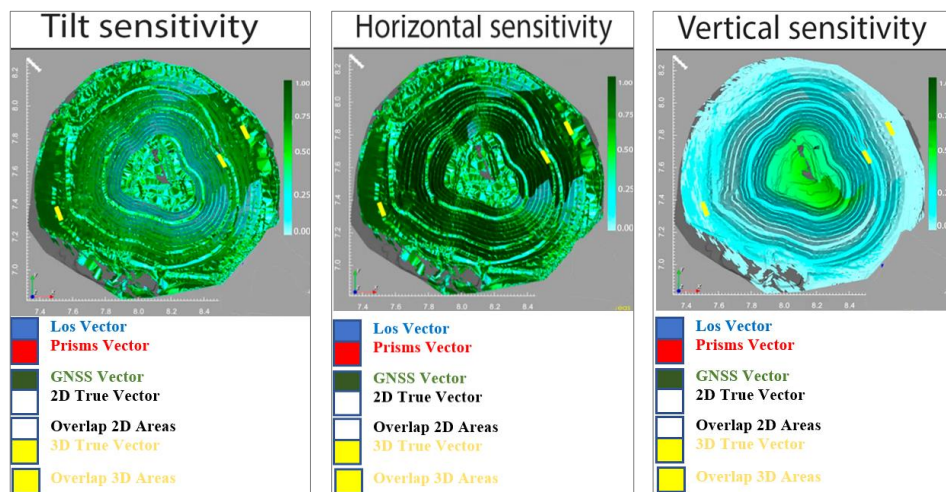


Figure 9. IBIS ArcSAR sensitivity map (FPM configuration)

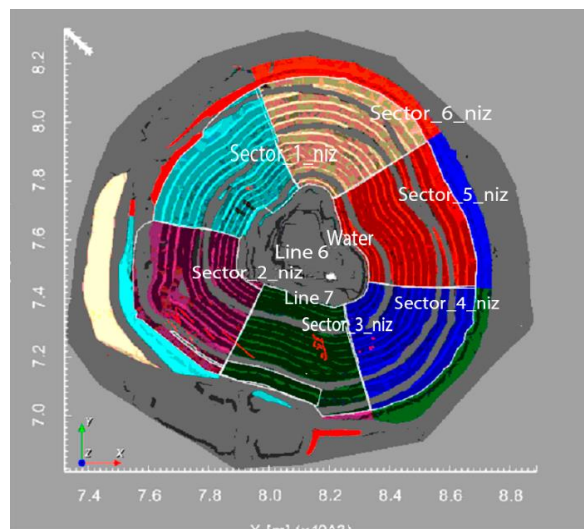


Figure 10. Sector diagram for the FPM 360 card and sector names

In this study, a sensitivity map was used to assess the correspondence of the GPR line of sight direction to the assumed array displacement vector. Figure 10 shows the results of sector modeling using the FPM 360 map. The map values range from 0 to 1: a value of 0 indicates minimum sensitivity (when the surface dip direction is perpendicular to the GPR line of sight), and a value of 1 indicates maximum sensitivity (when the dip direction is parallel to the GPR line of sight) (see Figures 11 to 14).

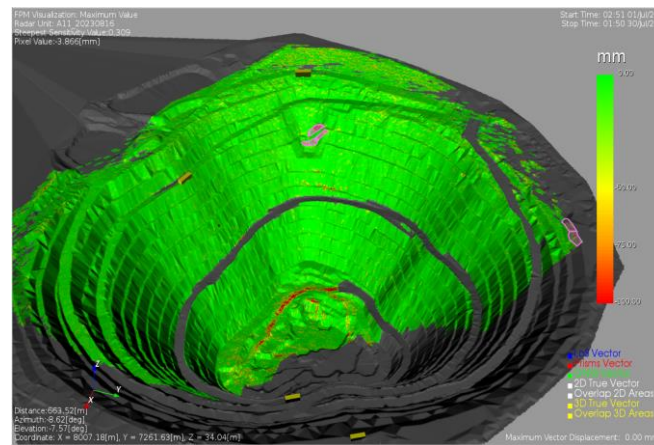


Figure 11. Displacement map and tectonic fault direction during 2023

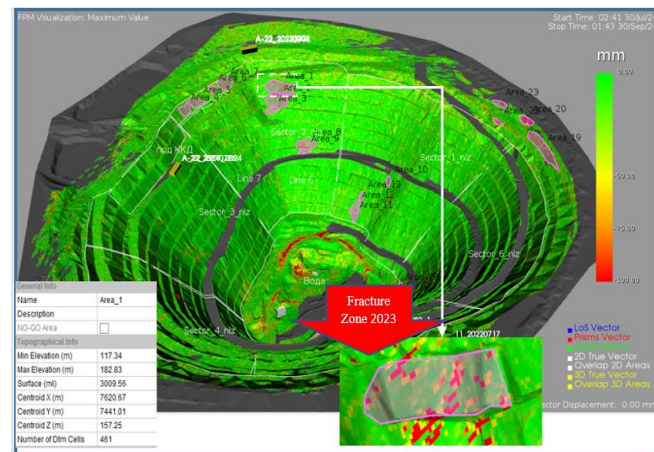


Figure 12. Displacements of the quarry face and in the fault zone and velocities with time, 2023

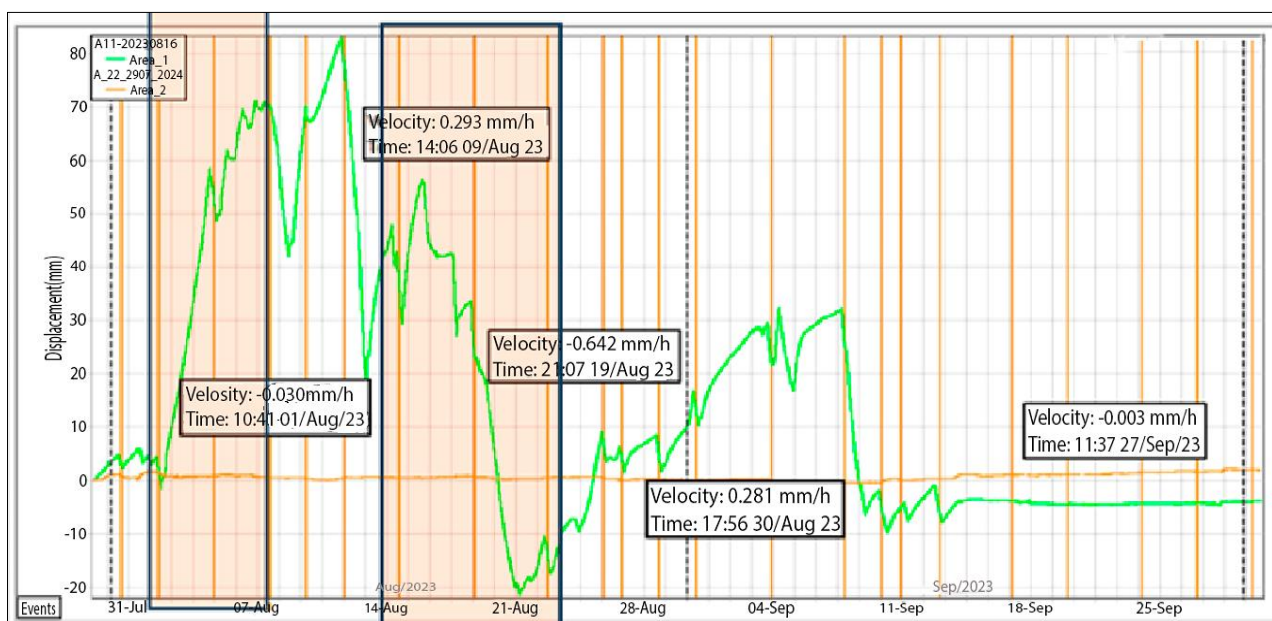


Figure 13. Results of displacement of the quarry face on sector No. 5 in 2023 (August used as a representative example)

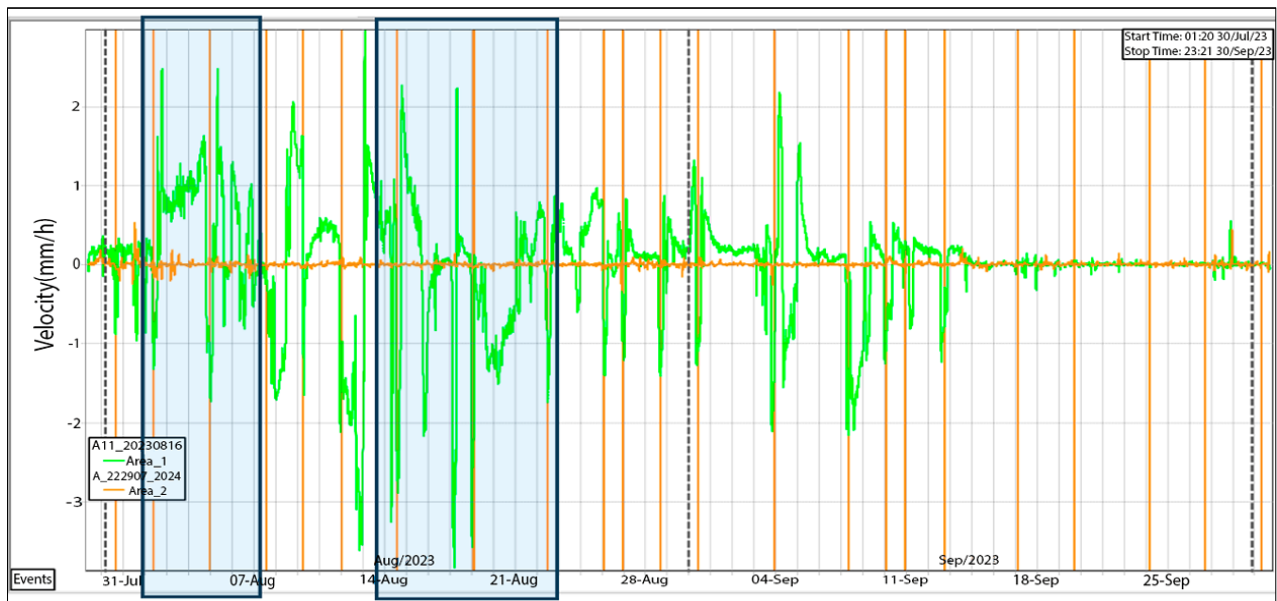


Figure 14. Results of pit face displacement as a function of velocity in sector No. 5 in 2024 (August used as a representative example)

The analysis revealed 16 sectors with varying degrees of potential hazard, among which sector No. 5 is of greatest interest. It was identified as the area with the highest geotechnical risk and requires additional detailed studies. Within this sector, a tectonic fault has been identified that significantly affects the nature and intensity of deformation processes in the rock mass. This circumstance must be taken into account when planning further mining operations to ensure the stability and safety of the developments.

Figure 13 illustrates the displacement of the quarry wall in sector No. 5 for August 2023, a month chosen as a representative period due to its high precipitation frequency. During the month, both gradual and abrupt changes in the deformation rate of the massif were observed. The initial stage (from August 1) is characterized by a slow displacement at a rate of -0.030 mm/h. The peak of activity was recorded on August 19, when the rate reached -0.642 mm/h, indicating rapid destruction in the instability zone. Between August 9 and 30, phases of both accelerated and slowed displacement were recorded, with deformations gradually stabilizing by the end of the month. As of September 27, the rate had practically dropped to zero (-0.003 mm/h), indicating a transition to a stable state. Such fluctuations are associated with the influence of external climatic factors and require constant monitoring to prevent emergency situations.

Figure 14 shows the change in slope displacement velocity in sector No. 5 for August 2023, selected as a representative month due to high sedimentary activity in the study region. Between August 4 and 8 and August 13 and 21, intense fluctuations in velocity ranging from -3 to $+3$ mm/h were recorded, indicating an unstable state of the massif and active deformation processes. The data confirm the presence of unstable zones subject to accelerated displacement, probably due to over moistening of the rock. After August 25, a gradual decrease in the amplitude of fluctuations was observed, which may indicate a transition of the massif to a more stable state. The identified anomalies require regular monitoring and analysis of weather conditions for timely risk assessment.

Analysis of the data obtained in sector No. 5 in the period from 2023 revealed the presence of regressive-progressive deformation trends. According to the displacement plots, changes in the rate and magnitude of ground displacements were recorded, especially in the intervals from August 1 to 8 and from August 15 to 23, when the strain rate reached -3.774 mm/h. The maximum total displacement for this period amounted to -21.3 mm, which corresponds to the average level of geotechnical hazard (see Figures 15 to 17).

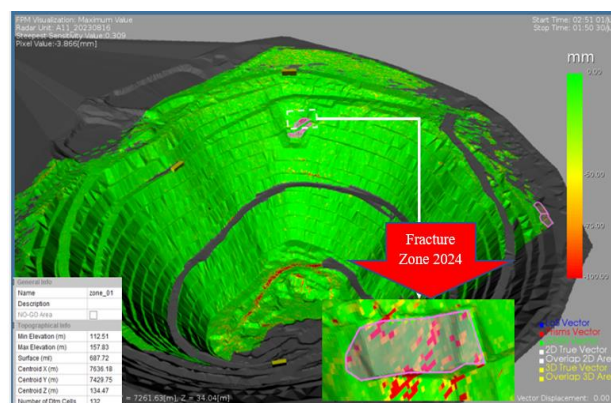


Figure 15. Displacements of the pit face and in the fault zone and velocity with time (2024)

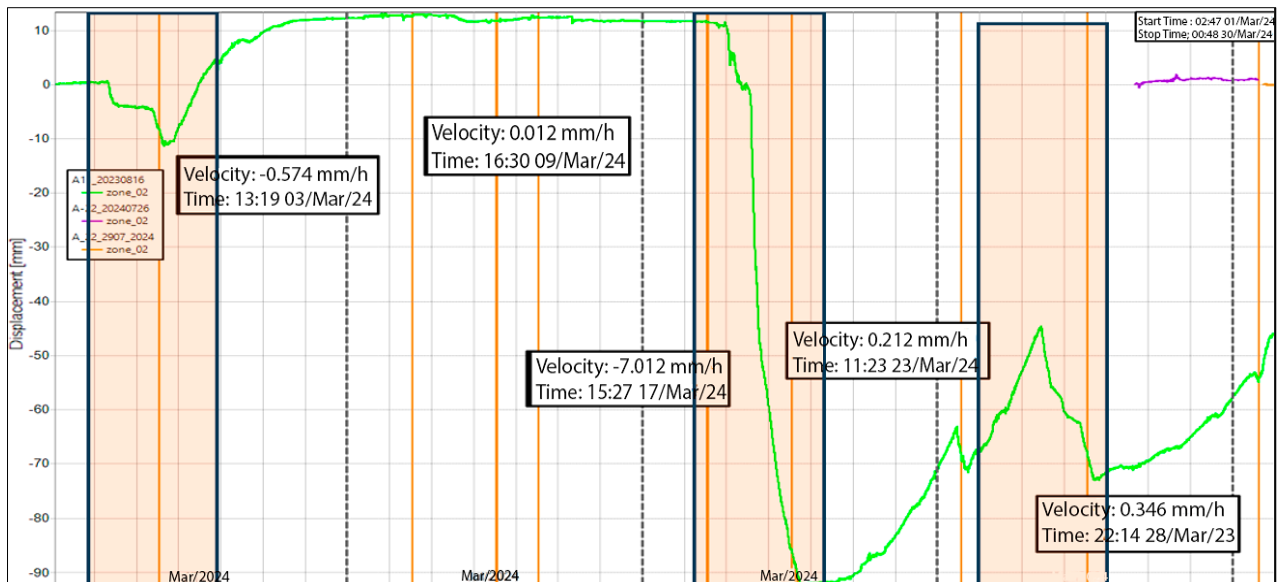


Figure 16. Results of displacement of the quarry face on sector No. 5 in 2024. (March used as a representative example)

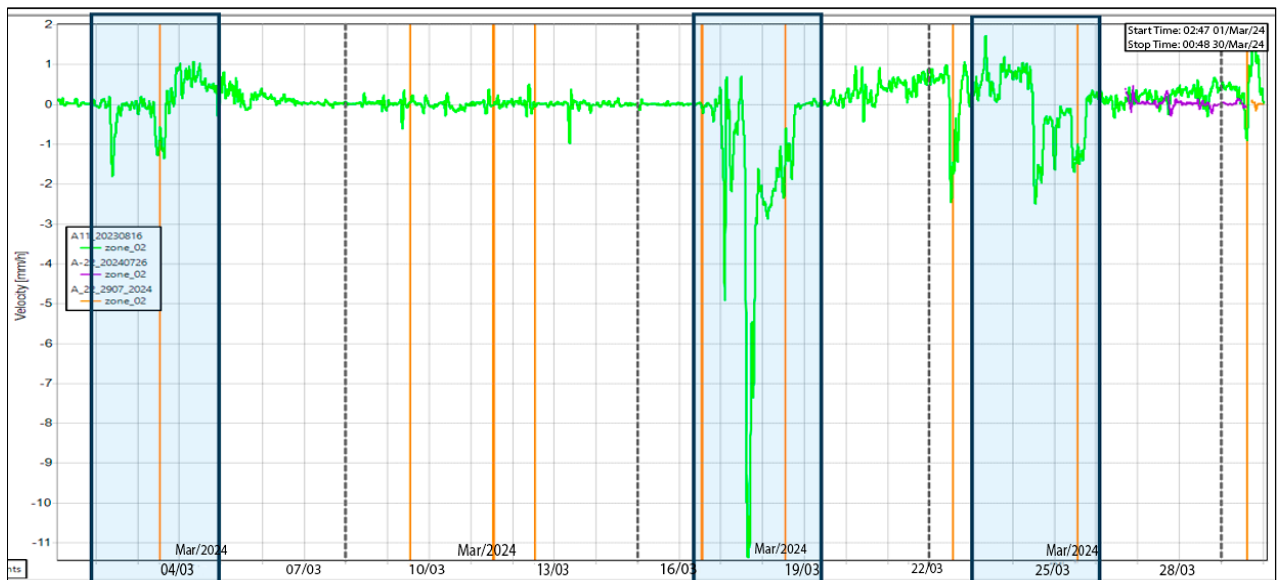


Figure 17. Results of pit face displacement as a function of velocity in sector No.5 in 2024. (March used as a representative example)

Figure 16 shows the dynamics of displacements in sector No. 5 for March 2024, based on GPR monitoring data. Several critical changes in displacement rates were recorded during the month. On March 3, a gradual displacement was observed at a rate of -0.574 mm/h (at 13:19), followed by a stable period with a minimum rate of 0.012 mm/h (March 9, 16:30). The most abrupt displacement occurred on March 17 at 15:27, when the speed reached -7.012 mm/h, indicating a sudden disturbance in stability. After that, the displacement was replaced by a growth phase: on March 23 (11:23), the rate was 0.212 mm/h, and by March 28 (22:14), it had increased to 0.346 mm/h. These data indicate the unstable state of the massif during the analyzed period and the need for immediate engineering and geotechnical intervention to prevent further deformation.

Figure 17 shows the results of the analysis of quarry wall displacements in sector No. 5 for March 2024, reflected in the form of changes in the deformation rate of the rock mass. The graph highlights three key periods of instability: March 4, March 18–20, and March 24–26. During these intervals, sharp negative peaks in velocity exceeding -10 mm/h were recorded, indicating sudden movements of the rock mass. Between the phases of activity, relatively stable sections were observed with fluctuations within ± 2 mm/h. These data confirm the presence of cyclic deformation dynamics characteristic of the transitional spring period, accompanied by increased humidity and thermal fluctuations. The results obtained require continued monitoring and the application of preventive measures to ensure the stability of the slopes.

In 2024, observations in sector No. 5 confirmed the preservation of regressive-progressive deformation trends. Changes in the ground velocity and displacement were recorded in the following periods: from March 3 to 5, from March 17 to 21 and from March 24 to 27. During these intervals, the strain rate reached -14.12 mm/h and the maximum displacement was -140.82 mm, indicating a high hazard level for this sector.

Thus, the results of the conducted monitoring and analysis indicate the need for continued monitoring and additional studies to assess slope stability and prevent potential threats to the safety of the quarry operation.

As a result of the conducted analysis of the data obtained in sector No. 5, the presence of regressive-progressive deformation trends was established, which were observed both in 2023 and 2024. In 2023, changes in ground velocity and displacement were recorded with a maximum displacement of -21.3 mm in the periods from August 1 to 8 and from August 15 to 23, which corresponds to the average hazard level. In 2024, although similar deformation trends were maintained, more significant changes were recorded: the rate of change reached -14.12 mm/h during the periods March 3 to 5, March 17 to 21, and March 24 to 27, with a maximum displacement of -140.82 mm, indicating a high hazard level for this sector.

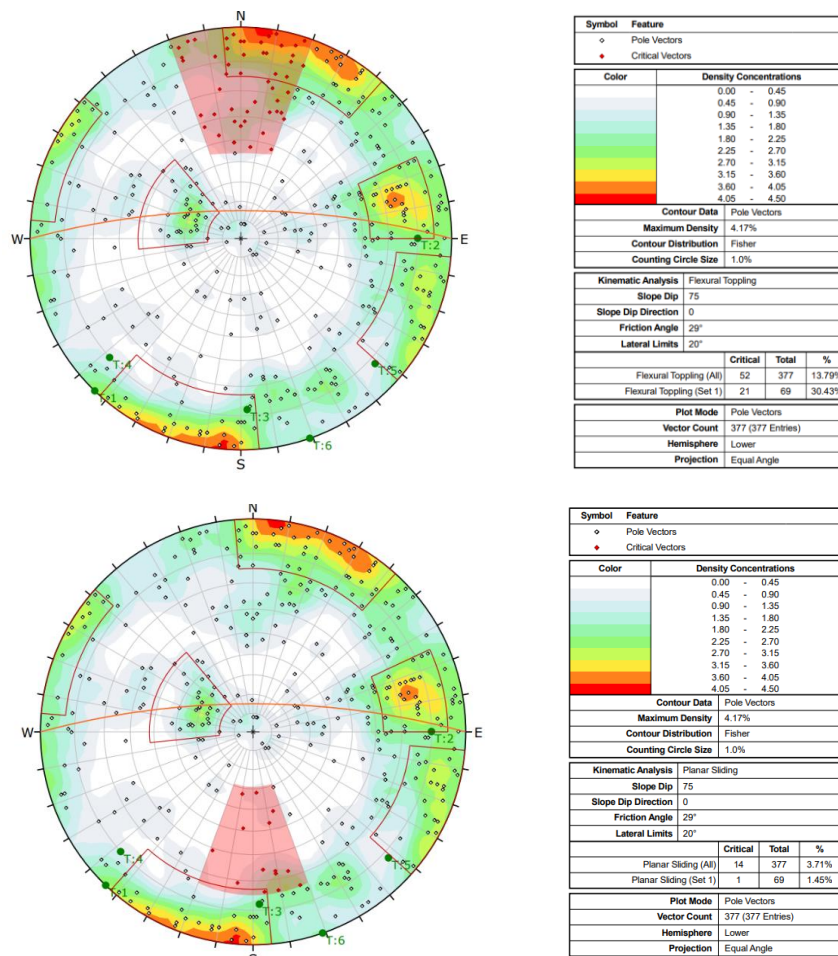
The observed deformation dynamics data were incorporated into the modeling of fracture direction using the DIPS program, which allowed for a more accurate definition of the controlled hazard zone and identification of the main fracture space systems affecting the stability of the massif. The results of the analysis will be used for further optimization of mining operations and development of measures aimed at ensuring safety at this section of the gold deposit.

4.2. Results of Modeling of Fracture Directions in the DIPS Program

To analyze tectonic faults, the Structural Interface tool of the RS2 software package was used, which allows for simulation of geological element interactions, considering fault structure and displacement potential along their boundaries. Tectonic faults are typically associated with zones of increased fracturing, which determine fault aperture, infill type, and surface roughness. These features are incorporated into the model using normal and shear stiffness parameters, which are essential for assessing massif stability in disturbed zones [26, 28, 29].

To enhance modeling reliability, all major quarry structures and physical-mechanical properties of both host and disturbed rocks were integrated into a finite element model [31, 33]. Analysis showed that tectonic activity significantly alters the strength parameters of rocks, reinforcing the importance of including such changes in engineering assessments.

A 3D geological model of the fault zone in Vasilkovskoye deposit was developed using Rocscience software. The model enabled a generalized evaluation of the geomechanical condition of the massif and identification of likely fracture propagation directions (Figure 18). This modeling approach supports safer and more efficient planning of drilling and blasting operations in complex geological settings.



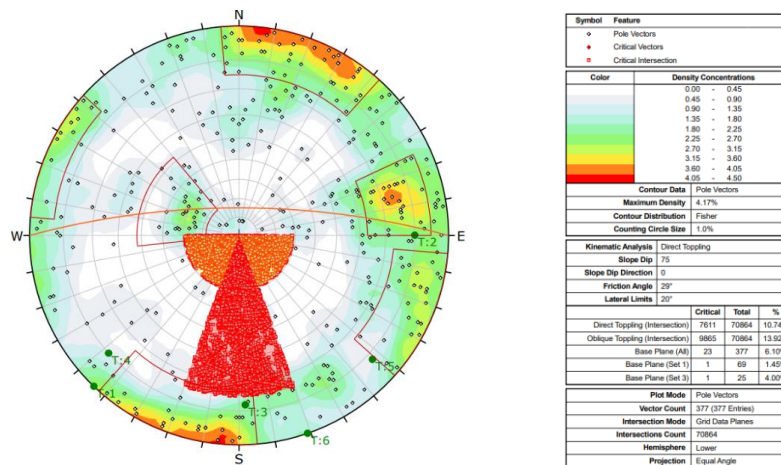


Figure 18. Diagram of spatial distribution of fracturing obtained as a result of modeling in the DIPS program

Figure 18 shows the spatial distribution of fracturing obtained as a result of modeling in the DIPS program. The diagram allows determining the prevailing directions of fractures and identifying areas of potential instability in the rock mass. Four primary discontinuity directions were identified: submeridional, sublatitudinal, northeastern, and northwestern. The most prominent direction is the northwestern strike-slip system, which is examined in detail in this study. The spatial orientation of fractures and tectonic disturbance trends informed the modeling of drilling and blasting parameters, aimed at optimizing stripping, ore block preparation, and ensuring operational safety at the gold deposit.

4.3. Results of Modeling of Drilling and Blasting Operations

Corresponding Modeling of drilling and blasting operations is essential for precise planning and optimization of rock fragmentation in modern mining. The integration of geotechnical monitoring, numerical simulation, and real-time rock mass data improves extraction efficiency while reducing environmental and operational risks [39-41]. Blasting parameters were developed using ShotPlus Premier 6 (Orica), enabling 3D modeling of drilling patterns, delay timing, and energy distribution, ensuring controlled fragmentation and effective breakage [42, 43]. Geological and tectonic features were closely considered. GPR data identified varying degrees of massif disturbance, with sector No. 5 marked by tectonic complexity that was selected for detailed modeling. This sector was subdivided into three zones: two in relatively stable rock with elevated risk, and one in a highly fractured block. For each, customized drilling and blasting passports were created, specifying hole geometry, charge structures, and delay sequences (Figures 19 and 20).



Figure 19. Site distribution at the actual quarry location

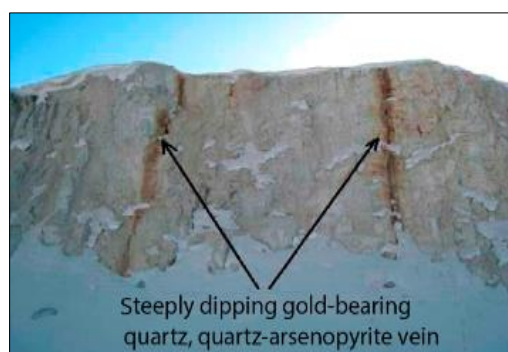


Figure 20. Scheme of directions and spatial location of tectonic faults in the territory of the study area

Modeling of rock movement directions based on tectonic data allowed for accurate localization of hazardous areas. These results guided the selection of charge types to ensure optimal fragmentation suitable for gold recovery. Magnetometric surveys confirmed major faults and revealed secondary faults with intense fracturing and inherited structural features. These were integrated into the blasting plan to improve safety and fragmentation quality (Figure 20).

4.3.1. Modeling of Drilling and Blasting Operations by Sections

A set of technical and economic calculations was performed to increase the efficiency of drilling and blasting operations (DBO) at the investigated sites. The optimal drilling and charging parameters were established based on the results of these calculations. As the main criterion of rationality, the ledge height is 7.5 m, which corresponds to the design length of wells. To ensure complete destruction of the massif, a 0.5 m deep over-drilling was envisaged, resulting in a total depth of the borehole reaching 8.0 m. The optimal well placement scheme varied depending on the geotechnical conditions at the sites: a 4.4×5.2 m grid was used at sites No. 1 and No. 2, while a denser 4.0×4.8 m grid was used at site No. 3. The choice of drilling grid parameters was conditioned by the geomechanical features of the rock mass, and by the requirements to the degree of rock mass crushing.

Ammonium nitrate-based granular mixture (ANFO) was used as the main explosive, which is characterized by high economic efficiency and reliability of application. The explosive consumption ($V_{explosive}$) per one meter of borehole was calculated by the formula.

$$V_{explosive} = \frac{\pi \cdot d^2}{4} \cdot \rho, \text{ kg} \quad (1)$$

where ($V_{explosive}$) is mass of explosive, kg – mass per unit length, i.e. per 1 meter, π – mathematical constant, d – borehole diameter, m, and ρ – explosive density, kg/m³.

The simulation results are presented in Tables 1 and 2, and visualized on the diagram, where the values of the main and additional explosives consumption for each section are shown. The analysis confirms the effectiveness of the selected parameters, providing uniform crushing of the array at minimum cost (Figure 21).

Table 1. Input data for modeling of drilling and blasting parameters for all investigated sites

| Parameters | Site No. 1 | Site No. 2 | Site No. 3 |
|--|------------|------------|------------|
| Well length, m | 7.5 | 7.5 | 7.5 |
| Depth of the drill, m | 0.5 | 0.5 | 0.5 |
| Well grid, m | 4.4×5.2 | 4.4×5.2 | 4.0×4.8 |
| Well diameter, m | 0.17 | 0.17 | 0.17 |
| Density of explosives, kg/m ³ | 880 | 880 | 880 |
| Consumption of explosives per 1 m, kg | 20 | 20 | 20 |
| Depth of the charged part, m | 6 | 6 | 6 |
| Total consumption of explosives per well, kg | 120 | 120 | 120 |
| Consumption of explosives for additional wells, kg | 40 | 40 | 40 |

Table 2. Main calculation indicators based on the results of modeling of DBO at the studied sites

| Key indicators | Types of blast hole | | |
|---|----------------------------|---------|---------|
| | Silence | Maximum | Minimum |
| <i>Study area No. 1</i> | <i>1st site</i> | | |
| Angle, (degree) | 0.0 | 5.0 | 0.0 |
| Line of least resistance LLR, (m) | 4.0 | 4.1 | 3.9 |
| Distances of least resistance of DLR, (m) | 4.8 | 4.9 | 4.7 |
| Charge location | Chess | | |
| Height of ledge, (m) | 7.5 | 7.6 | 7.4 |
| Over-drilling, (m) | 0.5 | 0.6 | 0.0 |
| Specific flow rate, (kg/m ³) | 0.90 | 0.99 | 0.00 |
| Hole, (m) | 2.0 | | |
| Side angle, (degree) | | 5.00 | 0.00 |
| Charging factor | 1.00 | | |
| Drill, (mm) | 115 | | |
| Length, (m) | 8.0 | | |

| Study area No. 2 | | 2 nd site | |
|---|-------|----------------------|------|
| Angle, (degree) | 0.0 | 5.0 | 0.0 |
| Line of least resistance LLR, (m) | 4.0 | 4.1 | 3.9 |
| Distances of least resistance of DLR, (m) | 4.8 | 4.9 | 4.7 |
| Charge location | Chess | | |
| Height of ledge, (m) | 7.5 | 7.6 | 7.4 |
| Over-drilling, (m) | 0.5 | 0.6 | 0.0 |
| Specific flow rate, (kg/m ³) | 0.90 | 0.99 | 0.00 |
| Hole, (m) | 2.0 | | |
| Side angle, (degree) | | 5.00 | 0.00 |
| Charging factor | 1.00 | | |
| Drill, (mm) | 115 | | |
| Length, (m) | 8.0 | | |
| Study area No. 3 | | 3 rd site | |
| Angle, (degree) | 0.0 | 5.0 | 0.0 |
| Line of least resistance LLR, (m) | 4.0 | 4.1 | 3.9 |
| Distances of least resistance of DLR, (m) | 4.8 | 4.9 | 4.7 |
| Charge location | Chess | | |
| Height of ledge, (m) | 7.5 | 7.6 | 7.4 |
| Over-drilling, (m) | 0.5 | 0.6 | 0.0 |
| Specific flow rate, (kg/m ³) | 0.90 | 0.99 | 0.00 |
| Hole, (m) | 2.0 | | |
| Side angle, (degree) | | 5.00 | 0.00 |
| Charging factor | 1.00 | | |
| Drill, (mm) | 115 | | |
| Length, (m) | 8.0 | | |

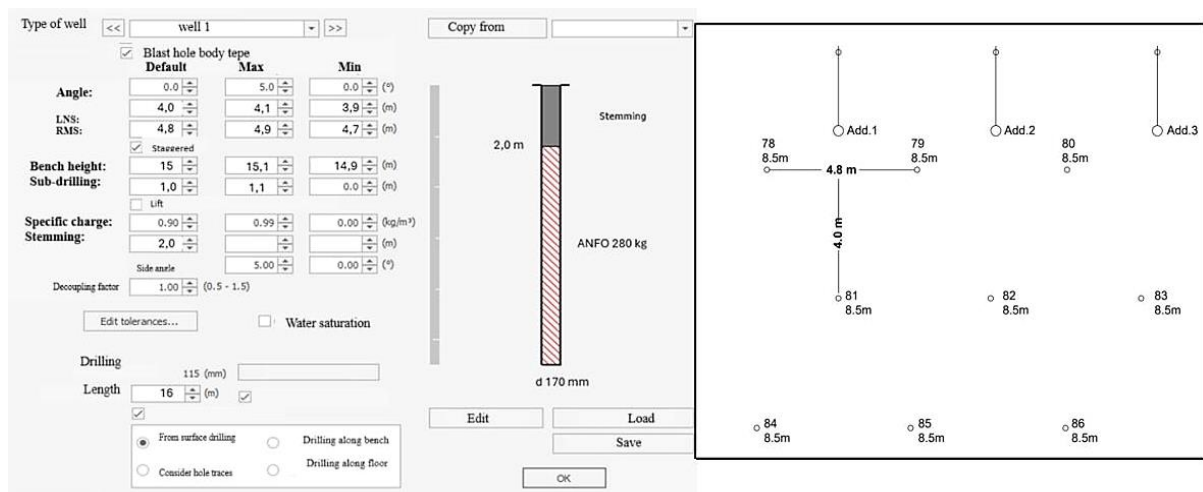


Figure 21. Results of modeling of drilling and blasting parameters for site No. 1

4.3.2. Blasting Installation and Preliminary Analysis of Rock Mass Fractional Composition

In sector No. 5, the drilling and blasting scheme remains unchanged, as the passport is developed with due regard to the spatial configuration and geotechnical conditions of the block. Figures 22 to 23 illustrate the cross-section of the charged block, the anticipated direction of rock movement, and a preliminary assessment of particle size distribution.

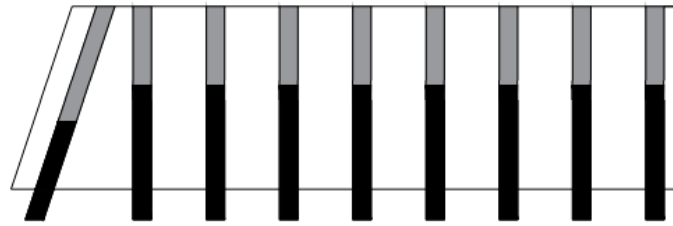


Figure 22. Sectional view of the blast block No. 465_007

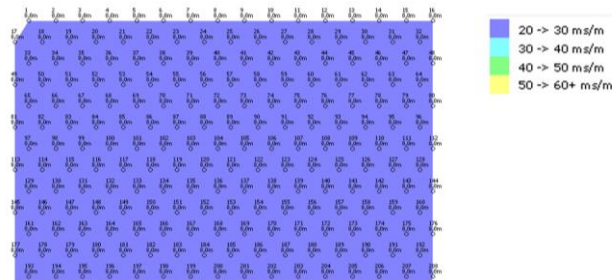


Figure 23. Preliminary analysis of the coarseness of the cut rock mass at the site No. 3

Using ShotPlus software, a forecast of post-blast fragmentation is conducted. If oversized fragments are predicted, design parameters can be promptly adjusted by introducing additional charge holes in critical zones. This approach enhances rock fragmentation efficiency, ensures optimal particle size for excavation and haulage, and reduces the load on primary crushers at the processing plant. Numerical modeling of drilling and blasting operations using ShotPlus software yielded preliminary estimates of rock mass particle size distribution within the target range of 200–600 mm. However, as the data are computational, they require validation through field observations. The current focus is on aligning actual fragmentation results with design specifications. This requires a detailed analysis of charge structure parameters and refinement of borehole charge configurations. Such optimization aims to enhance blast efficiency, improve rock fragmentation, and achieve the desired granulometric composition in the study area.

An analysis of meteorological and geotechnical data for 2023–2024 revealed a correlation between climatic factors and deformation activity in sector No. 5. August 2023 and March 2024 were selected as representative periods with the most pronounced weather fluctuations. In August, daily temperature fluctuations (20–30 °C), heavy precipitation (more than 15 mm/day after August 18), and gusty winds (up to 25 km/h) were accompanied by a sharp increase in displacement rates from 0.030 to 0.642 mm/h, indicating the activation of unstable areas of the massif. GPR surveying revealed areas of increased fracturing and local water saturation at a depth of 5–8 m, coinciding with areas of accelerated displacement. These data formed the basis of a refined geomechanical model, in which Midas GTS NX was used to simulate zones of concentrated shear stress (up to 1.8 MPa) at the boundaries of tectonic contacts. Calculations showed that under conditions of high humidity and temperature, the stability coefficient decreases from 1.28 to 0.96, approaching the pre-accident level.

The integration of ground-penetrating radar (GPR) systems, geomechanical modeling (RS2 and FLAC3D), digital blast planning (ShotPlus Premier), and ore redistribution analysis (OrePro 3D) has enabled the implementation of a complete closed-loop digital cycle for stability and blasting management. This solution demonstrates not only the technical feasibility of a comprehensive approach in complex tectonic conditions, but also its practical significance for increasing recovery, minimizing losses, and reducing geotechnical risks. As part of the simulation of transient processes caused by explosive loading, a sensitivity analysis of the FLAC3D model parameters was performed, including strength characteristics and contact zone stiffness parameters. The model was calibrated based on GPR and photogrammetry data. Variations in the normal stiffness modulus in the disturbance zones had the most significant impact on stability. The analysis confirmed the high sensitivity of the model's responses to fault geometry and weather conditions.

The GPR monitoring system operated continuously with data updates every 6 hours, enabling a near real-time feedback mechanism. When displacement thresholds (>3 mm/day) were exceeded, data was automatically transmitted for prompt correction of charging schemes. In particular, in August 2023, based on a sharp increase in the deformation rate (0.642 mm/h), the configuration of the boreholes was promptly changed and the charge density in unstable areas was reduced. This intervention prevented the collapse from developing and preserved the geometry of the bench. Adjusting the parameters of drilling and blasting operations based on the data obtained made it possible to reduce oversize volumes by 47% and residual stresses by 15%. Visual and radar monitoring confirmed the effectiveness of the changes. Unlike previous studies, this work is the first to implement a closed cycle: GPR monitoring, modeling, and

optimization of blasting parameters, which not only improves stability but also ensures economic feasibility. The results summarized in Table 3 clearly demonstrate that the presented work significantly expands the existing scientific and practical base and offers a comprehensive approach to solving the problems of stability, fragmentation, and optimization of drilling and blasting operations in complex tectonic conditions.

Table 3. Comparative contribution of the study

| # | Parameter | Previous Studies [3, 6, 10-14] | Present Study |
|---|--|--------------------------------|--|
| 1 | Continuous GPR monitoring | Partially implemented | Full integration |
| 2 | Tracking seasonal deformations | Not highlighted | Conducted with detail |
| 3 | Threshold values for displacement speeds | Not specified | Quantitatively determined (up to –14 mm/h) |
| 4 | Интеграция с цифровым моделированием BVR | Limited | Full closed loop |
| 5 | Verification of gold content increase | Rarely encountered | Confirmed (+9.59%) |
| 6 | Technical and economic analysis | Not sufficiently developed | Full justification |
| 7 | The relationship between tectonics and fragmentation | Presumptive | Quantitatively proven |

Continuous GPR monitoring. In a number of previous studies [3, 6, 10-14], ground-penetrating radar technologies were used to a limited extent — most often on a point-by-point basis, without systematic recording of changes over time. In this study, a full-fledged 24/7 monitoring system using A-22 and A-11 radars was implemented, providing high-precision observation of the state of the array at all stages of extraction. This made it possible not only to identify areas of instability, but also to construct real-time sensitivity and displacement maps. **Tracking seasonal deformations.** Unlike previous studies, in which climatic factors were taken into account after the fact or not considered at all, this study conducted a detailed analysis of seasonal changes. Critical weather conditions affecting stability (August 2023 and March 2024) have been identified, and the role of precipitation and temperature fluctuations in activating displacements has been confirmed, which is presented for the first time in a quantitatively verified form.

Threshold values of displacement velocities. Most published studies use qualitative characteristics of stability without specifying threshold values. This paper presents, for the first time, precise values of the limiting deformation rates of the rock mass (up to –14.12 mm/h), which allow formalizing the criteria for the transition from a stable to an unstable state of slopes. **Integration with digital modeling of blasting operations.** In previous publications, modeling of blasting operations was often considered in isolation from geomechanical and GPR data. This study demonstrates a closed digital loop in which monitoring results are immediately integrated into charging and optimization schemes via ShotPlus and OrePro 3D, allowing blast parameters to be quickly adapted to actual geological conditions.

Verification of gold content increase. In rare cases, quantitative assessments of the impact of charging schemes on the metal content in mined ore have been made in the literature. In our case, a production verification was performed, which showed an increase in the condition gold content by 9.59% due to a reduction in dilution and optimization of fragmentation. **Technical and economic analysis.** While most studies analyze the cost of various charging options superficially or not at all, this article presents a detailed comparative analysis that takes into account the cost of explosives, fragmentation efficiency, extraction, and long-term stability of slopes. This made it possible to justify the choice of a more expensive but technically justified option.

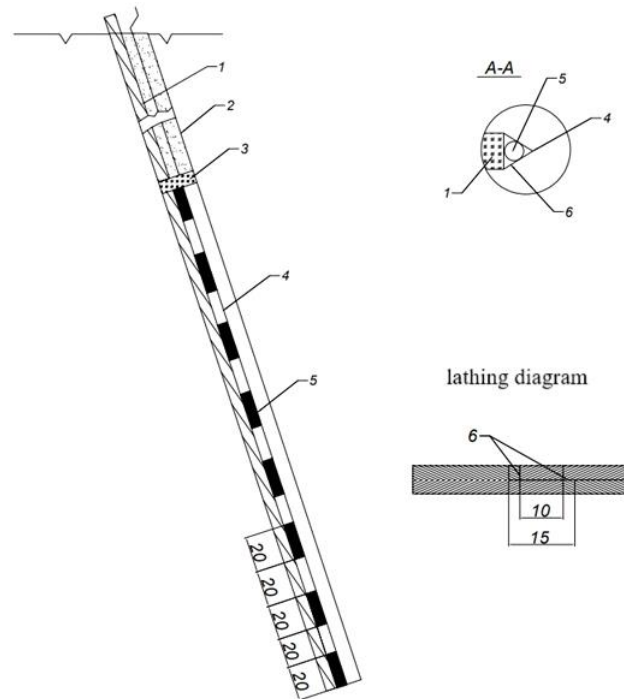
The relationship between tectonics and fragmentation. Many studies have asserted the influence of faults on the nature of rock mass failure, but such relationships are usually formulated at a qualitative level. This study established a quantitative relationship between fault orientation, displacement characteristics, and rock grain size distribution, which made it possible to adapt the charging parameters to specific tectonic conditions and increase the efficiency of the blast. The recommended comprehensive approach made it possible to identify the key factors of rock mass instability and propose sound engineering solutions to improve the safety and efficiency of work in structurally complex quarries.

5. Discussion

5.1. Comparative Analysis of Existing and Recommended Contour Drilling Method for Slope Stability

Ensuring slope stability is one of the key tasks in deep open-pit mining, especially at depths exceeding 500 m [44-46]. Proper design of bench geometry, slope angles, and pit contours is critical for minimizing landslide risks and technogenic deformations [47-49]. Within this study, an improved contour blasting method was developed for Site No. 5 to enhance pit wall stability by reducing damage beyond the design contour. Given the complex geological structure and location on the first mining level, special attention was paid to safe formation of contour benches. Design parameters

included a ledge height of 7.5 m and borehole depth of 8.2 m (including 0.5 m overdrilling). The spacing between contour holes was 1.5 m, while the distance to main holes ranged from 3.6 to 4.0 m. Senatel Powersplit ($\varnothing 45$ mm) was selected as the primary explosive, offering low dynamic impact and effective fragmentation with minimal disturbance. Implementation results of this method are shown in Figures 24 to 27.



1 - wooden lath (4,0x2,0 cm); 2 - borehole; 3 - paper plug; 4-DSE-12; 5 - BB cartridge weighing 300-600 g; 6 - twine.

Figure 24. Design solution of the inclined contour charge according to the approved project (on the rail)

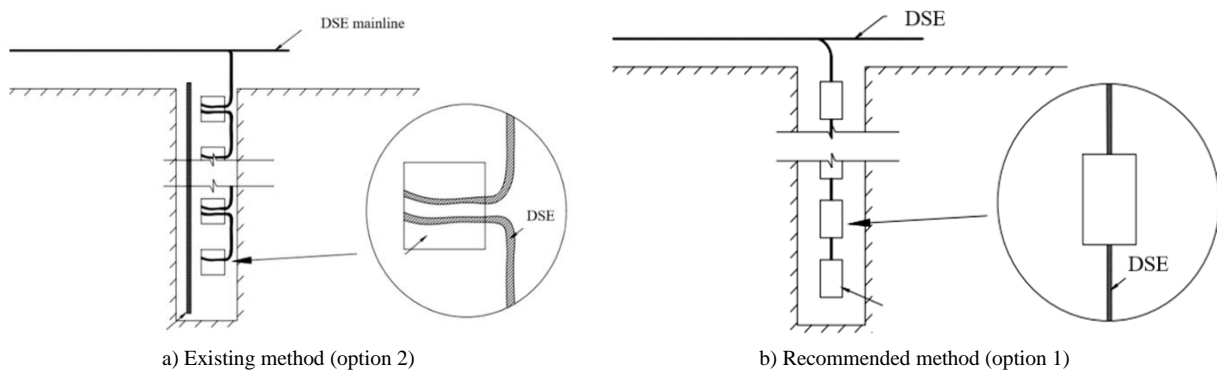


Figure 25. Explosive charge connection diagram for the recommended inclined contour charge design (DSE mainline)

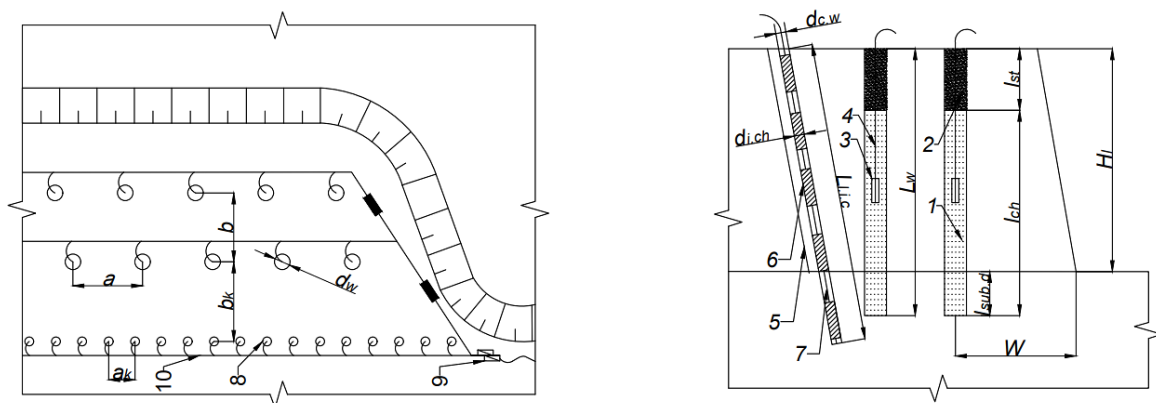
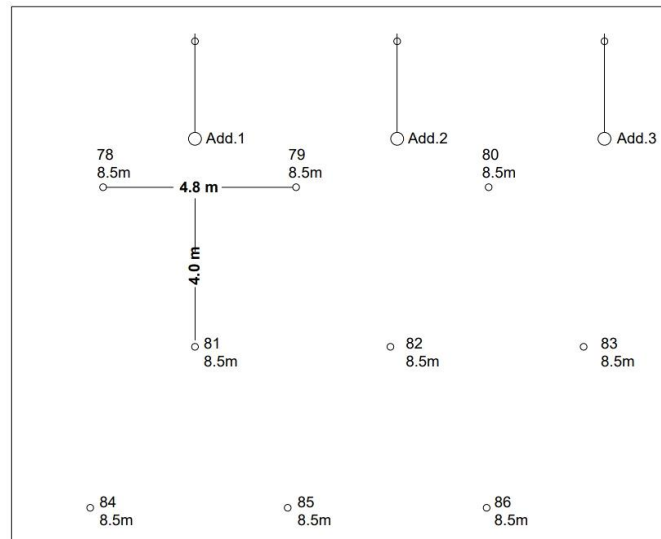


Figure 26. Drilling passport of the first scarp undercut together with contour wells



(1 - borehole ripping charge; 2 - bottom hole; 3 - warhead cartridge; 4 - DS; 5 - rock detachment line; 6 - contour charge; 7 - twine for cartridge fixing; 8 - contour well; 9 - ED; 10 - DS main line; a_k - distance between contour wells; a - distance between ripping wells; b_k - distance between rows of contour wells and ripping wells; b - distance between rows of ripping wells; W - line of resistance along the bottom, N_i - height of the ledge).

Figure 27. Schematic representation of wells position in the section

In accordance with the adopted system of field development, the site is mined in stages, by ledges, which meets modern requirements of rational subsoil use and ensuring the safety of mining operations. The contour wells are drilled to a depth of 8.2 meters, considering the necessary over-drilling, which ensures the required geometry of the ledge and compliance with the design parameters.

According to the developed passports of drilling and blasting operations, drawn up in compliance with the requirements of RK GOST "Blasting operations. General safety requirements" and RD 153-34.1-003-01, contour wells are drilled at the primary stage. After completion of drilling operations, the blasting cycle is conducted in strict accordance with the approved regulations, which allows to ensure control of seismic impact parameters and minimize damage to the massif outside the design contour.

Upon completion of the contour explosion, the next technological stage is implemented, the main boreholes 8 m deep are drilled. This sequence ensures structural stability of the massif and formation of a stable face, which is optimal for subsequent operations. The choice of these parameters is based on the results of preliminary engineering and geological studies, and on the tested process flow charts, confirmed by production practice at similar sites.

GPR monitoring at site No. 5 demonstrated the high efficiency of A-22 and A-11 systems. Sensitivity maps (Figures 7, 10-11) enabled localization and vector characterization of displacement zones. Unlike previous studies [20], this research introduced a sector-based analytical approach, improving the accuracy of stability assessments and enhancing sensitivity to local variations in the stress-strain state. Deformation analysis for 2023–2024 in sector No. 5 revealed alternating regressive-progressive trends, with maximum horizontal displacements reaching -140.82 mm in 2024, which exceeded values reported in [5, 21] and indicated elevated tectonic activity. These findings necessitate a revision of slope stability parameters for depths >500 m.

ShotPlus software was used for gradual adjustment of blasting parameters based on geomechanical data. Special emphasis was made on optimizing contour drilling at site No. 5 under high fracturing and tectonic stress. The designed ledge height was 7.5 m, with 8.2 m hole depth and 0.5 m over-drilling. The spacing between contour holes was reduced to 1.5 m, and the distance to main holes increased up to 4.0 m depending on local conditions.

Scientific contributions include:

- Integration of GPR, geomechanical, and numerical data;
- Use of sensitivity maps for predictive analysis;
- Stepwise adjustment of BPR parameters;
- Pre-drilling identification of high-risk zones;
- Optimization of contour drilling to minimize rock damage.

The proposed methodology enhances precision in risk identification, rationalizes drilling/blasting planning, and improves slope stability, which is particularly relevant for deep open pits. The positive results from sector No. 5 support its broader application in similar geological settings.

5.2. Analysis of Research Results

5.2.1. Control of Natural Size (Fractional Composition) of Rocks for Optimization of Gold Beneficiation Processes

The particle size distribution of rock mass is a critical factor in the efficiency of the “mining–crushing–beneficiation” chain in gold ore processing. Optimizing fragmentation at the drilling and blasting stage reduces energy consumption, enhances gold recovery, and minimizes losses of valuable components. Studies highlight the importance of monitoring and forecasting coarseness from explosive breakage to fine crushing [50].

Accurate granulometric control is essential for stable beneficiation. Mathematical modeling, digital monitoring, and blasting parameter optimization enhance productivity and process continuity. The transition to real-time adaptive control systems represents a key direction for sustainable gold mining [15, 51, 52].

At the Vasilkovskoye deposit, staged particle size control ensures process stability. Field sampling post-blasting in test zones (No. 1–No. 3) enables real-time assessment of lump sizes against design targets, directly influencing enrichment outcomes (Figure 28).

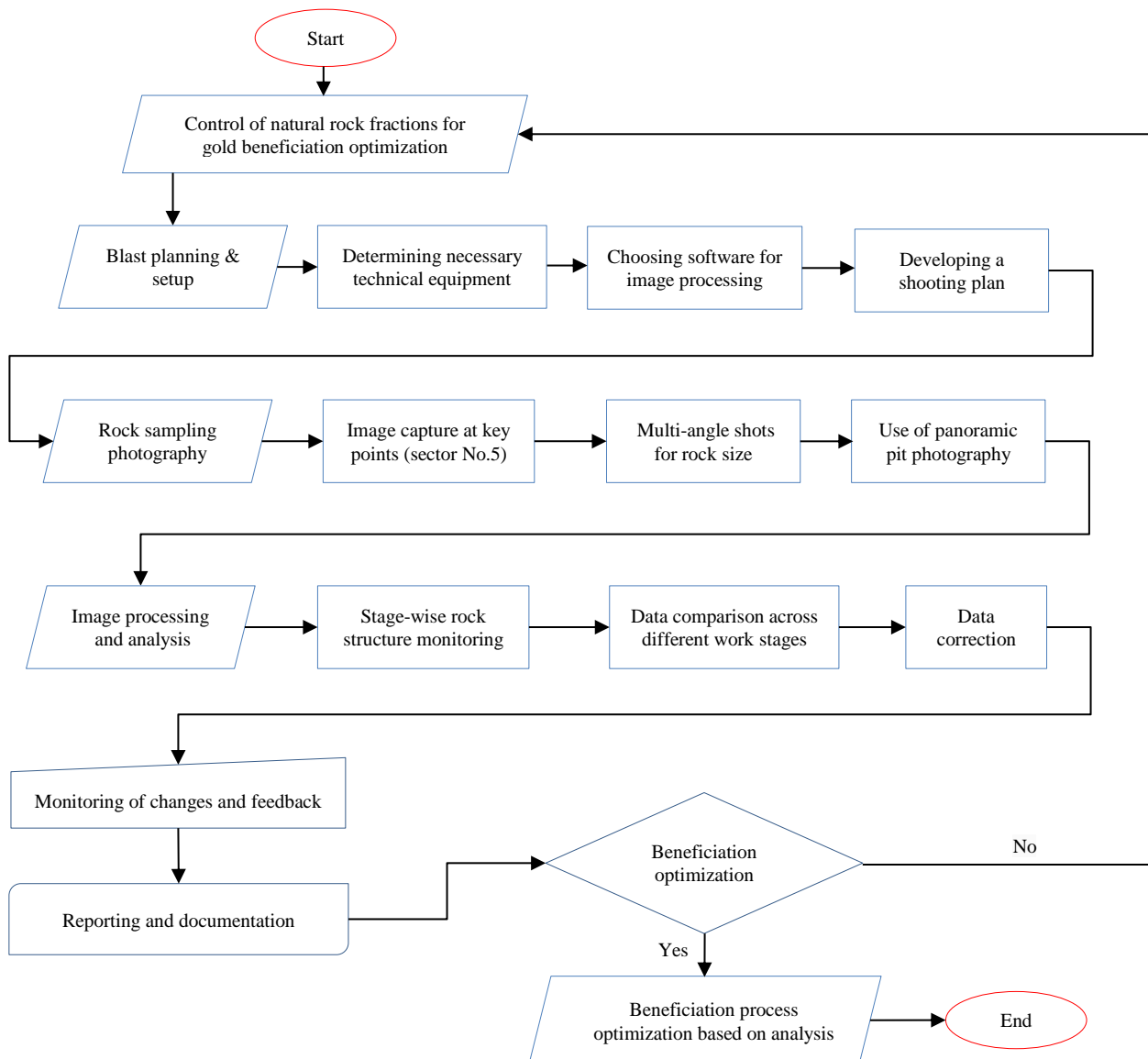


Figure 28. Rocks optimization of the gold enrichment process by controlling the natural size (fractional composition)

A detailed study of block No. 465_007 examined the relationship between particle size and tectonic fault orientation. Photographic analysis of sector No. 5 blasting, processed via AutoCAD and WinTopo, enabled granulometric evaluation and correlation with structural features, supporting the refinement of blasting parameters.

Figure 28 demonstrates the optimization of the gold extraction process by controlling the natural size (fractional composition) of the rock. The data presented shows that achieving the required fraction at the blasting stage reduces the load on crushing and grinding units and increases the efficiency of gravity and flotation enrichment.

Based on the results of the photo documentation, it is possible to distinguish rock coarseness, which on average varies from 20 mm to 750 mm (Figures 29 to 30). In the southwestern part of the ore field the faults are discontinuous, while towards the northeast they merge. These faults are generally accompanied by shallow zones of disturbance. One of such intersections, where the rocks have undergone minor crushing, is located near the Vasilkovskoye deposit [49].

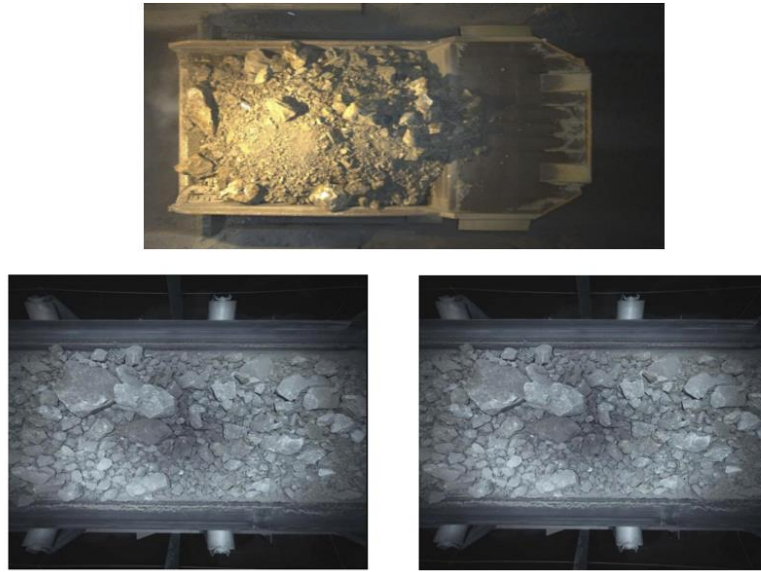


Figure 29. Fragments of photo documentation made during transportation of gold-bearing ores from the block No. 465_007

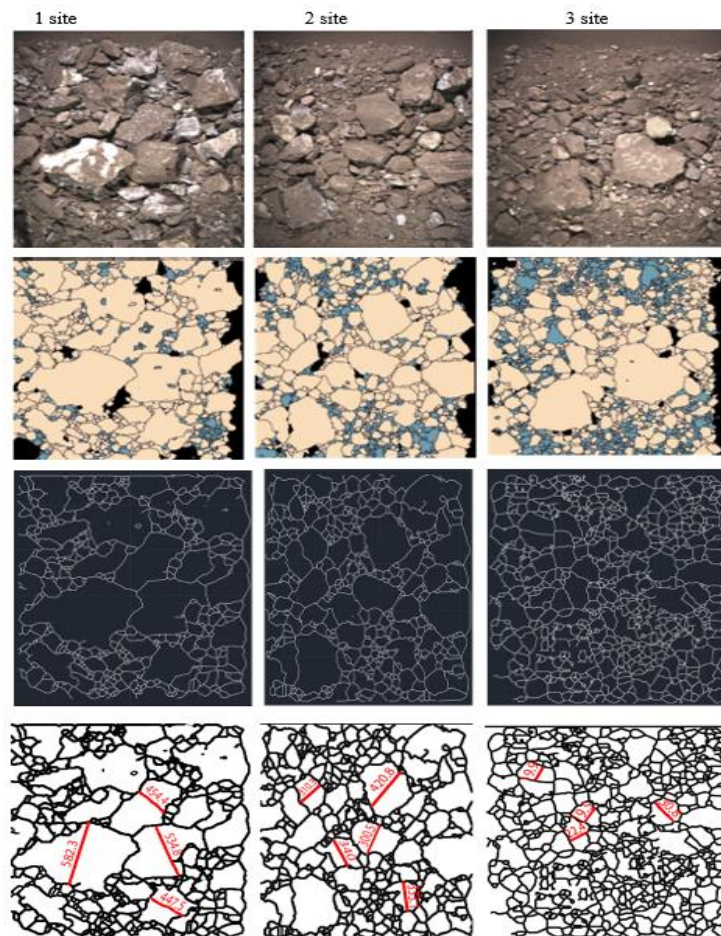


Figure 30. Sequence of studies to determine the fractional composition of rocks from block No. 465_007

The resulting rock mass was classified into fine (10–60 mm), medium (100–255 mm), and coarse (270–850 mm) fractions. The granulometric composition aligns with the predicted outcomes and complies with BWR passport specifications (see Figures 31 to 33).

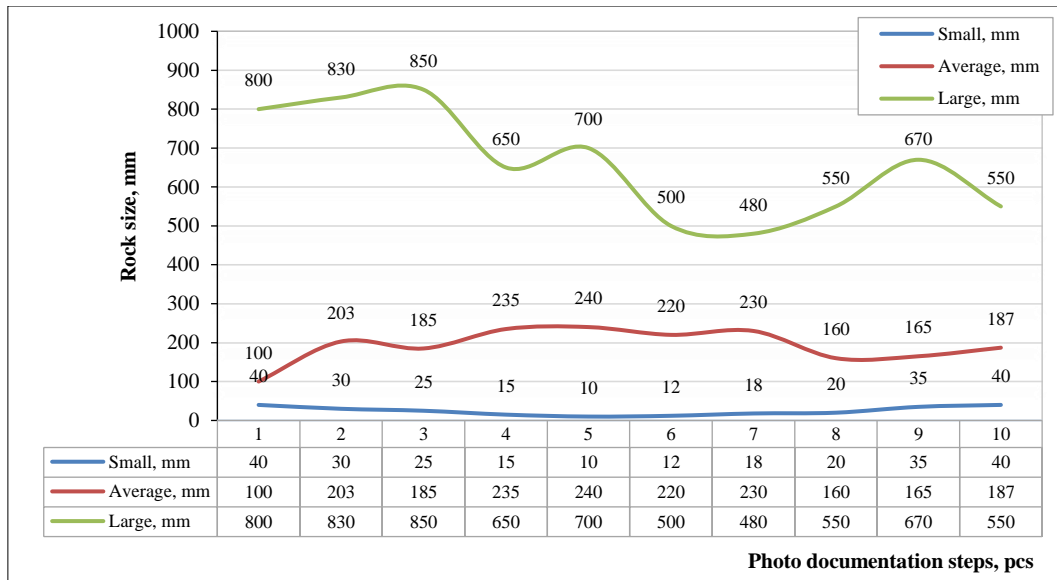


Figure 31. Results of rock coarseness (fractional composition) study at site No. 1

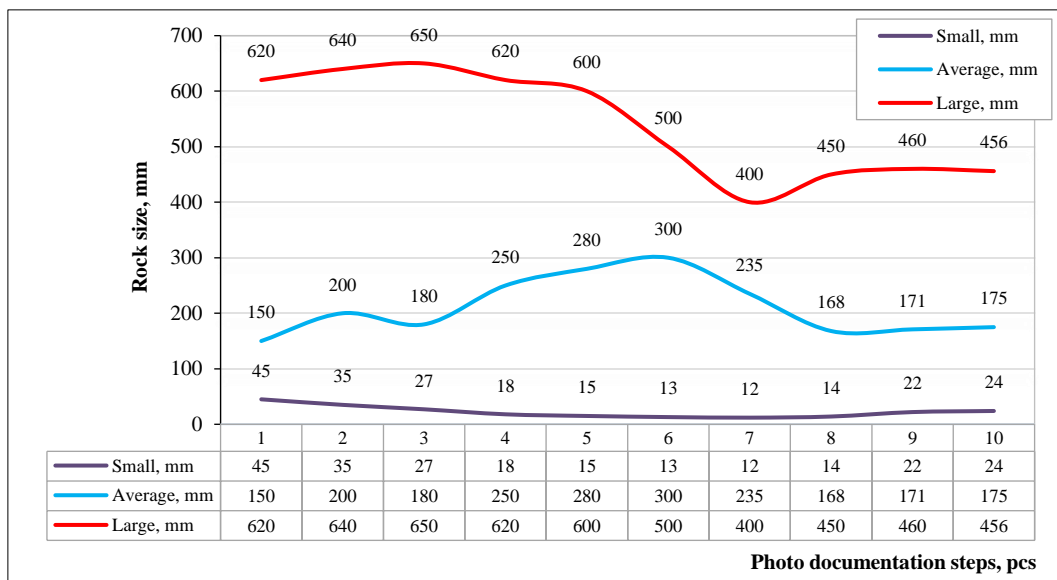


Figure 32. Results of rock coarseness (fractional composition) study at site No. 2

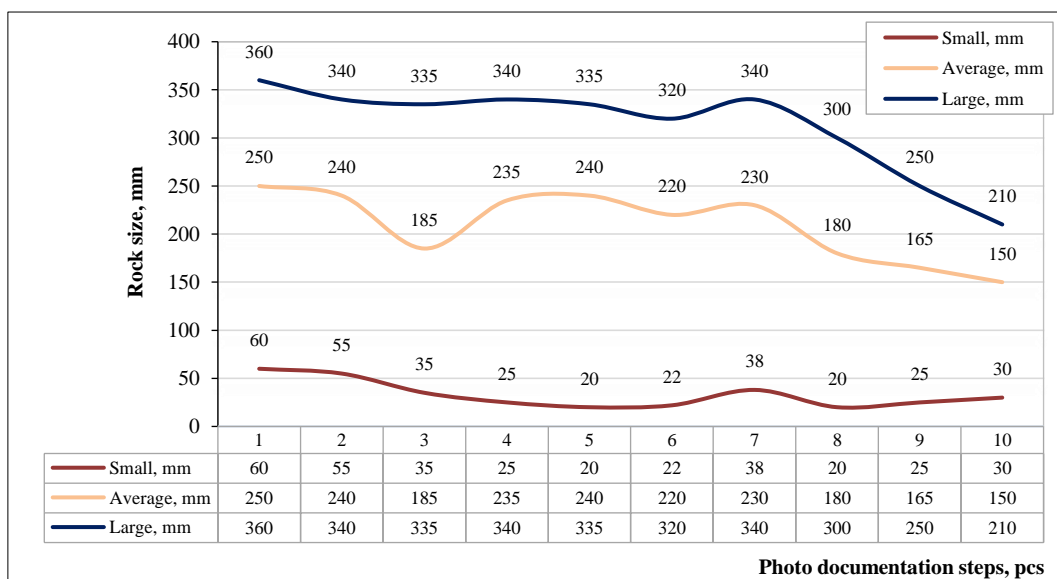


Figure 33. Results of rock coarseness (fractional composition) study at site No. 3

Figure 31 shows the results of the rock size (fractional composition) study at site No. 1. The graph reflects changes in the maximum, average, and minimum sizes of pieces as documented by photographs (10 observation steps). The average size ranged from 100 to 240 mm, the largest fraction reached 850 mm, and the small fraction remained in the range of 10–40 mm. There is a tendency toward a decrease in rock size toward the middle of the series of measurements, followed by a partial increase, which indicates the heterogeneity of crushing and the need to adjust the parameters of blasting operations.

Figure 32 illustrates the results of the analysis of rock size (fractional composition) at site No. 2. During the 10 steps of photo documentation, changes in fraction sizes were recorded: fine — from 45 to 12 mm, medium — from 150 to 300 mm, coarse — from 620 to 400 mm, with a subsequent increase to 456 mm. A regular decrease in fraction size is observed towards the middle of the observations, which may be due to improved crushing conditions, but a further increase in size indicates the instability of the process. The data obtained allow us to assess the effectiveness of drilling and blasting operations and the need to adjust them to achieve the required particle size distribution.

Figure 33 shows the results of the study of the fractional composition of rock in section No. 3. During the 10 stages of photo documentation, a general decrease in the size of all fractions was recorded. Large fractions decreased from 360 to 210 mm, medium fractions from 250 to 150 mm, and small fractions from 60 to 30 mm. The most uniform grinding dynamics were observed in comparison with other sites, which indicates the stability of drilling and blasting parameters and the effective organization of work. The final values indicate an approximation to the target size indicators for subsequent enrichment. Innovative approaches to optimizing gold beneficiation, incorporating GPR surveys, controlled blasting technologies, and integrated monitoring systems, markedly enhance mining efficiency. The combined application of these methods improves geological diagnostics of open pits, raises industrial safety standards, and ensures better mineral quality. The integration of GPR-based modeling, drilling and blasting simulation, and real-time monitoring establishes a foundation for safer and more productive gold extraction. This comprehensive strategy facilitates operational optimization and improves the overall economic performance of mining enterprises.

5.2.2. Comparative Economic Analysis and Impact on Gold Production Performance with Consideration of Dilution Reduction

As part of the evaluation of the proposed blasting method effectiveness, a comparative analysis of two options of its implementation was performed on the basis of technical and economic indicators. The first option envisaged blasting along the contour of the project block using a specially selected explosive with optimal characteristics to minimize the destruction of rocks outside the project contour. The second option was a more economical solution, using explosive materials available at the company without additional purchase of specialized compositions. To ensure a proper comparison of the effectiveness of both options, the estimated parameters of drilling and blasting operations were assumed to be identical – 50 holes in each case (see Table 4).

Table 4. Comparative technical and economic analysis of contour well blasting methods

| # | Material | Unit | Price per unit, tg | Cost of 2 options, tg | Cost of 1 option, tg |
|----------|---|------|--------------------|-----------------------|----------------------|
| 1 | Industrial explosive Magnum 50 | kg | 1000 | 400 000 | - |
| 2 | Electric detonator ED-8-Zh/ED-8-M1 L-2150 m | pcs | 845 | 845 | 845 |
| 3 | Detonating cord DSE-12 | m | 213 | 204 480 | 15 975 |
| 4 | Explosive wire vp 2×0.7 gost 6285-74 | m | 53 | 26 500 | 26 500 |
| 5 | Industrial explosive Senatel Powersplit | kg | 4500 | - | 2 925 000 |
| Total | | | | 631 825 | 2 968 320 |
| Variance | | | | 2 336 495 tg | |

Despite the apparent economic advantage of the second option (total cost 631,825 ₸ vs. 2,968,320 ₸ for the first), considering the geomechanical conditions of the deposit, the first option is more justified. The use of improved contour drilling and specialized explosives ensures the stability of pit slopes, which is critical in deformation-prone zones and helps reduce accident risks while extending the operational life of the quarry. Moreover, this blasting scheme provides the required granulometric composition, facilitating efficient loading, transportation, crushing, and beneficiation processes. Therefore, the first option is preferable based on a comprehensive technical, economic, and geomechanical evaluation.

OrePro 3D software was employed to enhance blast planning accuracy. Integrated into production workflows, it offers functionality for evaluating financial outcomes of various mining scenarios, particularly useful for structurally complex deposits. Developed in cooperation with major mining companies, OrePro 3D provides detailed modeling of rock mass displacement after blasting. It uses initial data such as blast designs, block models, and post-blast survey results to simulate ore redistribution and calculate displacement vectors, enabling accurate prediction of ore content in the post-blast rock mass [18, 19, 53].

An accurate understanding of the direction and nature of the displacement of the rock mass after blasting is of fundamental importance for effective separation of ore mass and waste rocks, and improvement of subsequent mining and processing operations effectiveness. This information is of significant value to the mining company, allowing it to minimize losses and dilution of ore.

Test drilling and blasting operations were performed in Block 465_007 to analyze and develop measures to reduce dilution at the site. All stages of design, calculations and subsequent modeling were performed using specialized ShotPlus and OrePro 3D software, which ensured high accuracy of both blasting preparation and evaluation of blasting results. The obtained data are visualized in Figure 34 and summarized in Table 5.

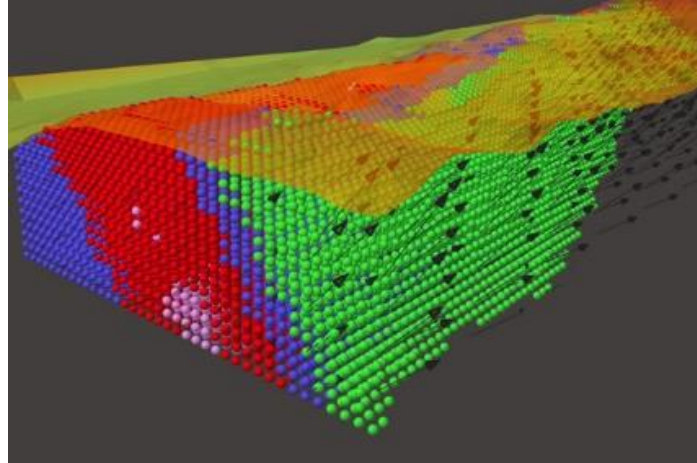


Figure 34. General position of the rock mass on the 3D image

Table 5. Total gold volume and grade in Block 465_007

| | Block 465_007 | | | |
|--------------|---------------|------|-------|----------|
| | Volume | Tons | Au | Metal |
| High Grade-1 | 1797.40741 | 4853 | 1.052 | 5105.356 |
| High Grade-2 | 40.3703704 | 109 | 1.049 | 114.341 |
| Total | 1837.77778 | 4962 | 1.052 | 5219.697 |

During test drilling and blasting in Block 465_007, an optimization system was implemented to reduce the dilution of the ore mass. The results confirmed the high efficiency of the proposed approach: precise planning and modeling using specialized ShotPlus and OrePro 3D software made it possible to achieve the planned parameters in terms of quality and control of ore mass redistribution.

Sector No. 5, monitored over two years, showed steady regression-progression dynamics, especially during transitional seasons. Analysis of meteorological and geomechanical data revealed a clear relationship between precipitation, thermal fluctuations, and array displacement rates. In March 2024, peak values of 14.12 mm/h and a cumulative displacement of -140.8 mm were recorded, which allowed the condition to be classified as a high level of geotechnical hazard. The article specifies the threshold values that separate medium from high risk 8 hours: the criteria are displacement rates >3 mm/h and cumulative displacements >100 mm over 5 days.

During the validation stage, a comparative assessment of fragmentation was carried out based on Shot Plus data and actual observations. Large oversized elements ($d > 700$ mm) were localized in areas of reduced fracture density identified during structural analysis (DIPS). Correlation analysis showed a relationship between the direction of tectonic fault extension and the nature of rock fragmentation ($R^2 = 0.79$), which indicates a quantitatively proven relationship between tectonics and fragmentation. The implementation of this methodology has helped improve the efficiency of mining operations and ore treatment performance, which in the long term positively influences the production results of the gold processing plant. In addition, optimization of drilling and blasting parameters allowed for reduction of depreciation expenses of the enterprise because of more rational use of equipment, materials and labor resources.

The results of OrePro 3D software implementation demonstrated a significant improvement in production performance. For example, in 2023, the gold grade in commercial ore before the application of digital modeling was 87.90%, while in 2024, after the implementation of the software, this indicator reached 97.49%. Thus, the increase in gold grade amounted to 9.59%, which demonstrates the high efficiency of integrating digital technologies into the technological chain of drilling, blasting and concentration processes (Tables 6 and 7).

Table 6. Reporting period 2023 before OrePro3D implementation

| Month | The fact of ore feed | | | Processing of GPP (gold processing plant) | | | Fulfillment, % |
|-----------|----------------------|---------|---------|---|---------|---------|----------------|
| | Volume | Au g/tn | Metal | Volume | Au g/tn | Metal | |
| August | 182 542 | 0.95 | 173 134 | 182 698 | 0.8 | 145 281 | 83.84 |
| September | 154 714 | 0.95 | 147 069 | 152 021 | 0.87 | 132 607 | 91.76 |
| October | 202 262 | 0.97 | 196 604 | 201 873 | 0.86 | 177 666 | 88.76 |
| November | 87 821 | 0.96 | 84 435 | 86 235 | 0.84 | 72 512 | 87.84 |
| December | 155 686 | 0.96 | 145 452 | 151 782 | 0.85 | 139 546 | 87.31 |
| Total | 783 025 | 0.96 | 746 694 | 774 609 | 0.84 | 667 612 | 87.90 |

Table 7. Reporting period 2024 after implementation of OrePro3D

| Month | The fact of ore feed | | | Processing of GPP (gold processing plant) | | | Fulfillment, % |
|----------|----------------------|---------|-----------|---|---------|---------|----------------|
| | Volume | Au g/tn | Metal | volume | Au g/tn | Metal | |
| January | 131 732 | 0.99 | 130 384 | 129 353 | 0.92 | 118 770 | 96.12 |
| February | 238 562 | 0.94 | 225 213 | 229 744 | 0.95 | 217 413 | 100.24 |
| March | 248 562 | 0.96 | 245 365 | 241 256 | 0.97 | 232 579 | 95.32 |
| April | 198 527 | 0.95 | 197 658 | 194 356 | 0.92 | 179 258 | 98.08 |
| May | 224 851 | 0.96 | 222 698 | 221 486 | 0.94 | 209 743 | 97.69 |
| Total | 1 042 234 | 0.96 | 1 021 318 | 1 016 195 | 0.94 | 957 763 | 97.49 |

The obtained results confirm the validity and expediency of the application of an integrated approach, including the use of GPR studies, modeling of drilling and blasting parameters and digital planning tools, to achieve the maximum degree of recovery of valuable components from ore raw materials and to ensure the sustainable development of a mining enterprise.

6. Conclusions

This study demonstrates that integrating real-time ground-penetrating radar (GPR), kinematic stereographic analysis, finite-element stress modeling and data-driven drill-and-blast optimization within a closed feedback circuit significantly improves technical performance and economic benefits in structurally complex open-pit gold operations. When applied to the fault-controlled Section No. 5 of the Vasilkovskoye deposit, the integrated workflow halved oversize generation, reduced dilution by almost one-third, raised the mill-feed grade from 0.84 g t^{-1} to 0.94 g t^{-1} and eliminated unplanned wall failures while simultaneously lowering unit mining costs. These results confirm that deformation dynamics and blast design are not independent engineering domains; rather when integrated they strengthen one another boosting productivity and safety.

The principal scientific contribution of the study lies in the formulation and industrial validation of a stepwise, tightly coupled methodology that joins four interdependent modules:

- GPR monitoring (IDS GeoRadar);
- Geomechanical characterization and kinematic analysis (RS2, DIPS);
- Numerical optimization of drill-and-blast parameters (ShotPlus Premier); and
- Real-time prediction and control of rock-mass fragmentation (OrePro 3D).

Tectonic fault orientations and displacement rates were measured and demonstrated a direct measurable impact on the size distribution of post-blast fragments for the first time in a single project; previously, similar studies had not reported such effect.

A comparison of two blasting methods (traditional with ANFO and adaptive with Senatel Powersplit) showed that despite the higher cost of the second option, it provides better crushing, slope stability, and, most importantly, a 9.59% increase in gold content, as confirmed by OrePro 3D data. This increase made it possible to increase the share of marketable ore from 87.9% to 97.49%, which is equivalent to a significant increase in production efficiency.

In addition, an analysis of economic sensitivity to external factors was conducted. When modeling scenarios of a 25% increase in the cost of BB and a simultaneous 12% drop in the price of gold, the project maintains positive profitability ($IRR \approx 18\%$), which confirms its stability and investment attractiveness.

Given the accumulated array of multi-parameter data, the authors consider the prospect of integrating machine learning (AI/ML) methods to predict areas of instability and assess the effectiveness of fragmentation. The use of XGBoost and Random Forest algorithms based on GPR data, structural analysis, meteorological observations, and charging parameters will enable the creation of an intelligent real-time decision support system.

Implementation at industrial scale (site 465_007) confirmed the practical efficacy of the model: specialized narrow-diameter explosives (Senatel Powersplit Ø45 mm), precise contour-hole design and refined drill patterns preserved slope stability and minimized ore losses, raising the saleable-ore gold grade from 87.90% in 2023 to 97.49% in 2024 (a 9.59% increase). These results highlight how digital technologies can be used to maximize metal recovery while also protecting geotechnical integrity.

Furthermore, this study contributes to a theoretical understanding of rock-mass behavior under active tectonics by determining the way in which structural anisotropies redistribute explosive energy and shape fragmentation outcomes. This granulometric process which is based on photogrammetry links fragment-size metrics to particular disturbance regimes enhancing the existing breakage theory. Additionally, the integrated stability-assessment system provides a transferable template for the design and operation of open pits in similarly complicated geomechanical settings by combining continuous GPR surveillance with high-fidelity numerical modeling.

However, two limitations hinder the applicability of the research results. First, the temporal and spatial scope is confined to a two-year window (2023–2024) and a single pit section, requiring further monitoring and modeling prior to projection to other domains. Second, the post-blast fragmentation estimates rely partly on software predictions that require further calibration against larger field sample sets. Wider adoption may also be limited by access to specialized explosives and advanced software in operations with different economic or geological contexts.

Future research should extend geomechanical monitoring over longer time horizons to record progressive stability trends and cumulative fragmentation changes. The integrated workflow should also be modified to other ore types (e.g., copper, polymetallic, or uranium) to test its universality. The research priorities include creating machine-learning modules for increased forecasting stability and improved fragmentation analysis, and implementing UAV-based machine-vision systems for automated high-resolution granulometric surveying.

Finally, energy-optimized, safety-centered blast designs should be further refined through systematic experiments on alternative charging schemes, explosive compositions and blast-induced seismic effects, particularly in highly tectonite media. These investigations will strengthen ore quality and operational reliability for a variety of mining environments.

7. Declarations

7.1. Author Contributions

Conceptualization, T.A., R.Z., and M.S.; methodology, T.A., R.Z., and M.S.; software, T.A. and R.Z.; validation, T.A. and R.Z.; formal analysis, T.A. and R.Z.; investigation, T.A. and R.Z.; resources, T.A. and R.Z.; data curation, T.A. and R.Z.; writing—original draft preparation, T.A., R.Z., and G.A.; writing—review and editing, T.A., R.Z., G.A., and N.A.; visualization, T.A., R.Z., and S.A.; supervision, T.A. and R.Z.; project administration, T.A. and R.Z.; funding acquisition, T.A. and R.Z. All authors have read and agreed to the published version of the manuscript.

7.2. Data Availability Statement

The data presented in this study are available in the article.

7.3. Funding and Acknowledgements

The authors acknowledge the financial support provided by the Committee of Science of the Ministry of Science and Higher Education of the Republic of Kazakhstan under research Grant No. AP23488914, which funds the project “Development of technology for quantitative assessment of finely dispersed gold in natural and man-made objects and assessment of the prospects for its detection in the territory of Kazakhstan”.

7.4. Conflicts of Interest

The authors declare no conflict of interest.

8. References

- [1] Mcevoy, D. (2025). What's the latest with the gold race rally? MoneyWeek, London, United Kingdom. Available online: https://moneyweek.com/investments/commodities/gold/gold-price?utm_source=chatgpt.com (accessed on November 2025).
- [2] Perincek, O., Loxton, R., Kulkarni, S., & Arthur, D. (2025). Drill Pattern Optimisation for Large Complex Blasts to Improve Fragmentation and Dig Efficiency. *Mathematical Geosciences*, 57(3), 577–599. doi:10.1007/s11004-024-10174-1.
- [3] Yu, K., Lin, P., Chitombo, G., Ma, L., & Peng, C. (2024). Study on the optimization of blasting parameters and blastholes charging structure for broken orebody. *Tunnelling and Underground Space Technology*, 152, 105948. doi:10.1016/j.tust.2024.105948.
- [4] Serdaliyev, Y., Bakhramov, B., & Alip, A. (2025). Improvement of blasting technology at gold-ore mining enterprises using contour blasting. *Mining of Mineral Deposits*, 19(2), 83–94. doi:10.33271/mining19.02.083.
- [5] Kgarume, T., van Schoor, M., & Nontso, Z. (2019). The use of 3D ground penetrating radar to mitigate the risk associated with falls of ground in Bushveld Complex platinum mines. *Journal of the Southern African Institute of Mining and Metallurgy*, 119(11), 973–982. doi:10.17159/2411-9717/603/2019.
- [6] Economou, N., Bano, M., & Ortega-ramirez, J. (2021). Delineation of fractures using a 2d GPR processing strategy for 3d imaging: Weak zones within carbonates at the archaeological site of xochicalco in Mexico. *Applied Sciences (Switzerland)*, 11(13), 5893. doi:10.3390/app11135893.
- [7] Luo, G., Cao, Y., Xu, H., Yang, G., Wang, S., Huang, Y., & Bai, Z. (2021). Research on typical soil physical properties in a mining area: Feasibility of three-dimensional ground penetrating radar detection. *Environmental Earth Sciences*, 80(3), 92. doi:10.1007/s12665-021-09383-2.
- [8] Manu E, Preko K, & Wemegah DD. (2013). Application of Ground Penetrating Radar in delineating zones of Gold Mineralization at the Subenso-North Concession of Newmont Ghana Gold Limited. *International Journal of Scientific and Research Publications*, 3(5), 1–11.
- [9] Zhang, Q., Zhang, H., Wang, L., Li, Q., & Yu, H. (2024). Effect of structural characteristics on the stability of multi-weak rock slopes considering the spatial variability of geotechnical parameters. *Scientific Reports*, 14(1), 30618. doi:10.1038/s41598-024-82296-9.
- [10] Ullah, S., Ren, G., Ge, Y., & Kinyua, E. M. (2025). Evaluation and Prediction of Blast-Induced Ground Vibration Using Gaussian Process Regression at Saindak Copper–Gold Open Pit Mine, Pakistan. *Mining, Metallurgy & Exploration*, 42(1), 155–170. doi:10.1007/s42461-024-01159-z.
- [11] Zvarivadza, T., Yi, C., Dineva, S., Onifade, M., Khandelwal, M., & Genc, B. (2025). Evaluating destress blasting for rock fracture and rockburst prediction in deep level hardrock mining. *Journal of the Southern African Institute of Mining and Metallurgy*, 125(6), 273–298. doi:10.17159/2411-9717/3685/2025.
- [12] Li, Z. (2023). Rock mass characterization using ground penetrating radar (GPR), rotary-percussion drilling performance, and indentation test. Ph.D. Thesis, Memorial University of Newfoundland, St. John's, Canada.
- [13] Arthur, C. K., Temeng, V. A., & Ziggah, Y. Y. (2020). Novel approach to predicting blast-induced ground vibration using Gaussian process regression. *Engineering with Computers*, 36(1), 29–42. doi:10.1007/s00366-018-0686-3.
- [14] van Schoor, M., Nkosi, Z., Magweregwede, F., & Kgarume, T. (2022). *Deep-Level Gold and Platinum Mining*. Springer International Publishing, Cham, Switzerland. doi:10.1007/978-3-031-09491-0.
- [15] Rysbekov, K., Nurpeisova, M., Kassymkanova, K. K., Meirambek, G., Kyrgyzbayeva, D., & Rakhimbayeva, D. (2025). Providing Stability of Quarry Slopes At Combined Mining of Mineral Deposits. *Naukovyi Visnyk Natsionalnoho Hirnychoho Universytetu*, 2(2), 60–68. doi:10.33271/nvngu/2025-2/060.
- [16] Wu, X., Zhu, D., Lu, H., & Li, L. (2024). Simulation research on blasting of an open pit mine slope considering elevation conditions and slope shape factors. *Frontiers in Earth Science*, 12, 1417895. doi:10.3389/feart.2024.1417895.
- [17] Kuciewicz, M., Łukasz, M., Baranowski, P., Małachowski, J., Fuławka, K., Mertuszka, P., & Szumny, M. (2024). Numerical modeling of blast-induced rock fragmentation in deep mining with 3D and 2D FEM method approaches. *Journal of Rock Mechanics and Geotechnical Engineering*, 16(11), 4532–4553. doi:10.1016/j.jrmge.2024.01.017.
- [18] Ming, J., Pan, Y., Xie, J., Li, Z., & Guo, R. (2024). Study on the law of ore dilution and loss and control strategies under brow line failure in sublevel caving mining. *Scientific Reports*, 14(1), 26195. doi:10.1038/s41598-024-77064-8.
- [19] Hmoud, S., & Kumral, M. (2025). Risk-Based Optimization of Post-Blast Dig-Limits Incorporating Blast Movement and Grade Uncertainties with Multiple Destinations in Open-Pit Mines. *Natural Resources Research*, 34(1), 193–214. doi:10.1007/s11053-024-10428-z.
- [20] Orient Exploration Team LLP. (2022). Report on Mineral Resources and Mineral Reserves for Open Pit Mining of the Vasilkovskoye Gold Deposit in accordance with KAZRC Standards. Orient Petroleum Inc., Astana, Kazakhstan.

- [21] Torbica, S., & Lapcevic, V. (2014). Rock breakage by explosives. *European International Journal of Science and Technology*, 3(2), 96-104.
- [22] Al-Mistarehi, B., Imam, R., Al-Shawabkah, M. M., Shtayat, A., & Al-Omari, A. (2024). Assessing the Effect of Geometric Design and Land Use on Roundabouts Using Video Camera. *Civil Engineering Journal*, 10(11), 3626–3639. doi:10.28991/CEJ-2024-010-11-012.
- [23] Almenov, T., Zhanakova, R., Sarybayev, M., & Shabaz, D. M. (2025). A Novel Approach to Selecting Rational Supports for Underground Mining Workings. *Civil Engineering Journal (Iran)*, 11(3), 1217–1241. doi:10.28991/CEJ-2025-011-03-022.
- [24] Zhou, J., Gao, S., Luo, P., Fan, J., & Zhao, C. (2024). Optimization of Blasting Parameters Considering Both Vibration Reduction and Profile Control: A Case Study in a Mountain Hard Rock Tunnel. *Buildings*, 14(5), 1421. doi:10.3390/buildings14051421.
- [25] Kaiser, P. K., & McCreath, D. R. (1994). Rock mechanics considerations for drilled or bored excavations in hard rock. *Tunnelling and Underground Space Technology*, 9(4), 425–437. doi:10.1016/0886-7798(94)90101-5.
- [26] Wang, R., & Elmo, D. (2024). Discrete Fracture Network (DFN) as an Effective Tool to Study the Scale Effects of Rock Quality Designation Measurements. *Applied Sciences (Switzerland)*, 14(16), 7101. doi:10.3390/app14167101.
- [27] Zaid, M., & Sadique, M. R. (2021). The response of rock tunnel when subjected to blast loading: Finite element analysis. *Engineering Reports*, 3(2). doi:10.1002/eng2.12293.
- [28] Etemadifar, M., Shoaie, G., Javadi, M., & Hashemnejad, A. (2025). A Developed Computational Code to Build a 3D Fracture Network to Reduce the Uncertainty of Fracture Parameter Generation (A Case Study of the Emamzadeh Hashem Tunnel). *Geosciences (Switzerland)*, 15(1), 6. doi:10.3390/geosciences15010006.
- [29] Chen, N., Liu, Z. W., Xiao, H. L., & Li, L. H. (2025). UAV-Based Simulation of 3D Random Discontinuity Networks in Rock Slopes. *Geotechnical and Geological Engineering*, 43(1), 16. doi:10.1007/s10706-024-02997-w.
- [30] Shields, L., Silva, J., Calnan, J., Maldonado, E., & Agioutantis, Z. (2025). Integrating Underground Blast Fragmentation Modeling for Sustainable Mine-to-Mill Optimization: A Focus on Blast Fragmentation and Energy Efficiency in Comminution Circuits. *Rock Mechanics and Rock Engineering*, 58(4), 4497–4508. doi:10.1007/s00603-024-04118-8.
- [31] Zhao, Y., Hua, W., Chen, G., Liang, D., Liu, Z., & Liu, X. (2021). New method for estimating strike and dip based on structural expansion orientation for 3D geological modeling. *Frontiers of Earth Science*, 15(3), 676-691. doi:10.1007/s11707-021-0903-z.
- [32] Hu, B., Zhang, Q., Li, S., Yu, H., Wang, X., & Wang, H. (2022). Application of Numerical Simulation Methods in Solving Complex Mining Engineering Problems in Dingxi Mine, China. *Minerals*, 12(2), 123. doi:10.3390/min12020123.
- [33] Alipenhani, B., Amnieh, H. B., & Majdi, A. (2022). Physical model simulation of block caving in jointed rock mass. *International Journal of Mining and Geo-Engineering*, 56(4), 349–359. doi:10.22059/IJMG.2022.339663.594953.
- [34] Department of Mines, Industry Regulation and Safety. (2019). Ground control management in Western Australian mining operations—guideline. Department of Mines, Industry Regulation and Safety, East Perth, Australia. Available online: https://www.worksafe.wa.gov.au/system/files/documents/2025-02/MSH_GL_GroundControl.pdf (accessed on July 2025).
- [35] Masoumi, I., Zabihi, B., & Masoumi, S. (2024). Optimizing Rock Fragmentation in Open-Pit Mines Through Fuzzy Intelligent Prediction Method. *Mining Science*, 31, 21–38. doi:10.37190/msc243102.
- [36] Weir Motion Metrics. (2020). *TruckMetrics and CrusherMetrics: Solutions for Optimizing Blasting Operations*. Weir Motion Metrics, Vancouver, Canada.
- [37] Motion Metrics. (2020). *Introducing BeltMetrics™ Volume Monitoring*. Motion Metrics, Vancouver, Canada. Available online: <https://www.motionmetrics.com/introducing-beltmetrics-volume-monitoring/> (accessed on November 2025).
- [38] Hong, Z., Tao, M., Zhao, M., Zhou, J., Yu, H., & Wu, C. (2023). Numerical modelling of rock fragmentation under high in-situ stresses and short-delay blast loading. *Engineering Fracture Mechanics*, 293, 109727. doi:10.1016/j.engfracmech.2023.109727.
- [39] Aruna, M., Vardhan, H., Tripathi, A. K., Parida, S., Raja Sekhar Reddy, N. V., Sivalingam, K. M., Yingqiu, L., & Elumalai, P. V. (2025). Enhancing safety in surface mine blasting operations with IoT based ground vibration monitoring and prediction system integrated with machine learning. *Scientific Reports*, 15(1), 3999. doi:10.1038/s41598-025-86827-w.
- [40] Yang, Q., Gao, Q., Jia, Y., Zhou, H., Gao, X., Jiang, W., & Ma, X. (2025). Application of Simulation Methods and Image Processing Techniques in Rock Blasting and Fragmentation Optimization. *Applied Sciences (Switzerland)*, 15(6), 3365. doi:10.3390/app15063365.
- [41] Deressa, G. W., & Choudhary, B. S. (2025). Evaluating Productivity in Opencast Mines: A Machine Learning Analysis of Drill-Blast and Surface Miner Operations. *Natural Resources Research*, 34(1), 215–251. doi:10.1007/s11053-024-10429-y.

- [42] Abbaspour, H., Drebenstedt, C., Badroddin, M., & Maghaminik, A. (2018). Optimized design of drilling and blasting operations in open pit mines under technical and economic uncertainties by system dynamic modelling. *International Journal of Mining Science and Technology*, 28(6), 839–848. doi:10.1016/j.ijmst.2018.06.009.
- [43] Karlsen, J., & Rigby, S. E. (2024). The role of AI in engineering: Towards rapid inverse blast analysis. *Proceedings of The 4th International Conference on Structural Safety Under Fire & Blast Loading (CONFAB 2024)*, 9-10 September, 2024, London, United Kingdom.
- [44] Eremenko, A. A., Konurin, A. I., Shtirts, V. A., & Volkov, A. V. (2024). Features of rock mass geodynamics during large-scale blasting in rockburst-hazardous iron ore mining. *Gornyi Zhurnal*, 1, 50–56. doi:10.17580/gzh.2024.01.08.
- [45] Deressa, G. W., Choudhary, B. S., & Jilo, N. Z. (2025). Optimizing blast design and bench geometry for stability and productivity in open pit limestone mines using experimental and numerical approaches. *Scientific Reports*, 15(1), 5796. doi:10.1038/s41598-025-90242-6.
- [46] Begalinov, A., Khomiakov, V., Serdaliyev, Y., Iskakov, Y., & Zhanbolatov, A. (2020). Formulation of methods reducing landslide phenomena and the collapse of career slopes during open-pit mining. *E3S Web of Conferences*, 168, 6. doi:10.1051/e3sconf/202016800006.
- [47] Lu, Y., Jin, C., Wang, Q., Han, T., Zhang, J., & Chen, L. (2023). Numerical study on spatial distribution of blast-induced damage zone in open-pit slope. *International Journal of Rock Mechanics and Mining Sciences*, 163, 105328. doi:10.1016/j.ijrmms.2023.105328.
- [48] Almenov, T., Begalinov, A., Serdaliev, E., Amanzholov, D., Zhaksybek, B., and Bakhramov B. (2015) Method of development of steeply falling vein deposits. (Kazakhstan Patent No. 30460). National Institute of Intellectual Property of the Republic of Kazakhstan, Korgalzhyn, Kazakhstan. Available online: <https://kz.patents.su/4-ip30460-sposob-razrabotki-krutopadayushhih-zhilnyh-mestorozhdenijj.html> (accessed on November 2025). (In Russian).
- [49] Begalinov, A., Almenov, T., Zhanakova, R., & Bektur, B. (2020). Analysis of the stress deformed state of rocks around the haulage roadway of the beskempir field (Kazakhstan). *Mining of Mineral Deposits*, 14(3), 28–36. doi:10.33271/mining14.03.028.
- [50] Zhang, Z. X., Sanchidrián, J. A., Ouchterlony, F., & Luukkanen, S. (2023). Reduction of Fragment Size from Mining to Mineral Processing: A Review. *Rock Mechanics and Rock Engineering*, 56(1), 747–778. doi:10.1007/s00603-022-03068-3.
- [51] Borodin, A. A., Kabulova, E. G., & Polozhentsev, K. A. (2016). Video detection of problems in the melting of consumable electrodes in a vacuum arc furnace. *Steel in Translation*, 46(5), 322–324. doi:10.3103/S0967091216050041.
- [52] Posphehov, G. B., Norova, L. P., & Izotova, V. A. (2024). Comparing the methods of grain size analysis of gypsum-containing sulfuric acid wastes neutralized with limestone. *Sustainable Development of Mountain Territories*, 16(4), 1729–1742. doi:10.21177/1998-4502-2024-16-4-1729-1742.
- [53] Orica (2023). Blast Movement Modeling with OREPro 3D – Case Study: Touquoy Mine, St Barbara. Orica Technical Papers. Orica Ltd, Victoria, Australia. Available online: https://www.orica.com/ArticleDocuments/2605/5000109_Touquoy%20Mine%2C%20St%20Barbara%20Case%20Study.pdf.aspx (accessed on November 2025).